

AD-R126 543

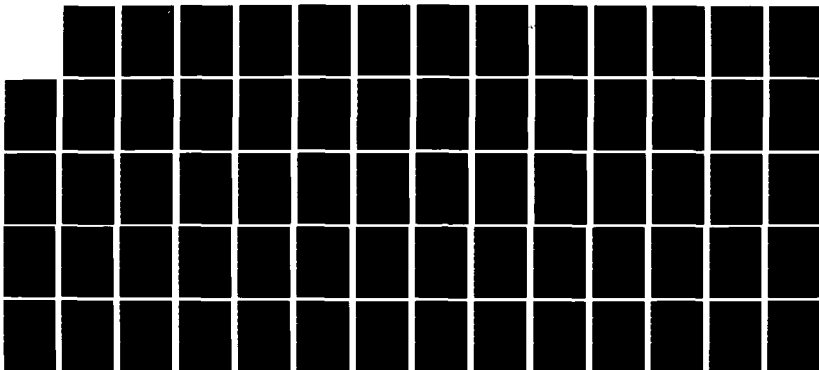
THE EFFECTS OF IRON OXIDATION STATE ON CLAY SWELLING
(U) ILLINOIS UNIV AT URBANA DEPT OF AGRONOMY
J W STUCKI 07 MAR 83 ARO-16797.3-GS DAAG29-80-C-0004

1/1

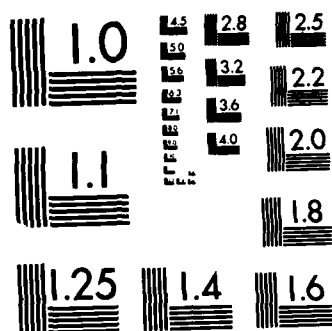
UNCLASSIFIED

F/G 8/7

NL



END



ARO 16797.3-GS

(12)

ADA 126543

THE EFFECTS OF IRON OXIDATION STATE
ON CLAY SWELLING

Final Report

Joseph W. Stucki

7 March 1983

U. S. Army Research Office

Contract NO. DAAG29-80-C-0004

University of Illinois

The view, opinions, and/or findings contained in this report are those of the author and should not be construed as an official Department of the Army position, policy, or decision, unless so designated by other documentation.

DTIC FILE COPY

Approved for Public Release;
Distribution Unlimited

DTIC
APR 7 1983
A

83 04 07 097

Unclassified

-11-

SECURITY CLASSIFICATION OF THIS PAGE (When Data Entered)

REPORT DOCUMENTATION PAGE		READ INSTRUCTIONS BEFORE COMPLETING FORM
1. REPORT NUMBER	2. GOVT ACCESSION NO. AD-A126543	3. RECIPIENT'S CATALOG NUMBER
4. TITLE (and Subtitle) THE EFFECTS OF IRON OXIDATION STATE ON CLAY SWELLING		5. TYPE OF REPORT & PERIOD COVERED Final Report
		6. PERFORMING ORG. REPORT NUMBER
7. AUTHOR(s) Joseph W. Stucki		8. CONTRACT OR GRANT NUMBER(s) DAAG29-80-C-0004
9. PERFORMING ORGANIZATION NAME AND ADDRESS University of Illinois, Department of Agronomy, S-510 Turner Hall, 1102 South Goodwin Avenue, Urbana, IL 61801		10. PROGRAM ELEMENT, PROJECT, TASK AREA & WORK UNIT NUMBERS IL161102 BH57-01 Atmos & Terr
11. CONTROLLING OFFICE NAME AND ADDRESS U. S. Army Research Office Post Office Box 12211 Research Triangle Park, NC 27709		12. REPORT DATE 7 March 1983
		13. NUMBER OF PAGES 65
14. MONITORING AGENCY NAME & ADDRESS (if different from Controlling Office) Office of Naval Research Branch Office Room 286, 536 South Clark St. Chicago, IL 60605		15. SECURITY CLASS. (of this report) Unclassified
		15a. DECLASSIFICATION/DOWNGRADING SCHEDULE
16. DISTRIBUTION STATEMENT (of this Report) Approved for public release; distribution unlimited.		
17. DISTRIBUTION STATEMENT (of the abstract entered in Block 20, if different from Report)		
18. SUPPLEMENTARY NOTES THE VIEW, OPINIONS, AND/OR FINDINGS CONTAINED IN THIS REPORT ARE THOSE OF THE AUTHOR(S) AND NOT NECESSARILY OF THE ARMY, THE NAVY, THE AIR FORCE, THE MARINE CORPS, OR THE DEPARTMENT OF DEFENSE, UNLESS SO DESIGNATED BY OTHER DOCUMENTATION.		
19. KEY WORDS (Continue on reverse side if necessary and identify by block number) Reduction, Oxidation, iron, clay, swelling, montmorillonite, nontronite, smectite, water, DLVO theory, surface charge, dissolution, methods, aluminum, silicon, inert atmosphere.		
20. ABSTRACT (Continue on reverse side if necessary and identify by block number) The effects of the state of iron oxidation in clay crystals on their swelling pressure and surface charge were investigated. The minerals studied were the < 2µm, Na⁺-saturated fractions of API 25 Upton (UPM), Czechoslovakia #650 (CZM), and New Zealand (NZM) montmo- rillonites, and API H-33a Garfield nontronite (GAN). Methods and appa- ratus were developed to prepare reduced suspensions in a pH-buffered		

DD FORM 1 JAN 73 1473

EDITION OF 1 NOV 65 IS OBSOLETE

Unclassified
SECURITY CLASSIFICATION OF THIS PAGE (When Data Entered)

20. ABSTRACT

medium, as is to remove the undesired solutes and to prepare dried, oriented clay films while minimizing reoxidation of the ferrous iron in the mineral structure.

In the composition range $0 < \text{Fe}^{2+} < 0.4 \text{ mmol/g clay}$, the surface charge increased linearly with ferrous iron composition according to the charge deficits created by the reduction of Fe^{3+} to Fe^{2+} . The swelling pressure decreased by 22%, 31%, 39%, and 56% for the respective clays UPM, CZM, GAN, and NZM containing 1.5 g $\text{H}_2\text{O/g}$ clay. Above this range, the surface charge deviated from the predicted relationship and the swelling pressure was largely unchanged. Upon reoxidation these effects were reversible.

TABLE OF CONTENTS

	Page
Report Documentation Page.....	ii
Table of Contents.....	iii
List of Appendixes, Illustrations, and Tables.....	iv
Introduction and Statement of Problem.....	1
Summary of Results.....	2
1. Methods, Techniques, and Apparatus.....	2
2. The Effect of CBD treatment and of Reoxida- tion on Surface Charge and Dissolution.....	17
3. The Effect of Iron Oxidation State on Clay Swelling.....	27
4. The Relation Between c-axis Spacings and Water Contents of Clay Gels at Various Applied Swelling Pressures.....	43
List of Publications.....	45
Participating Scientific Personnel	
Bibliography.....	47
Appendixes.....	50



A

LIST OF APPENDIXES, ILLUSTRATIONS, AND TABLES

	Page
<u>Appendixes</u>	
A. The Quantitative Assay of Minerals for Fe^{2+} and Fe^{3+} Using 1,10-Phenanthroline.....	50
1. Sources of Variability.....	51
2. A Photochemical Method.....	56
B. Potential Commercial Applications.....	60
<u>Illustrations</u>	
Figure 1.1 Schematic illustration of the reaction vessel used to prepare reduced smectite suspensions.....	5
Figure 1.2 Schematic drawing of the glass apparatus for deoxygenating solutions.....	7
Figure 1.3 Schematic drawing of the apparatus for exchanging and collecting supernatant solutions under an inert atmosphere. (For a more detailed view of the deoxygenating units see Fig. 1.2).....	8
Figure 1.4 Schematic drawing of the chamber used to prepare oriented films of reduced smectites.....	11
Figure 1.5 Fe^{2+} /total Fe ratios for 100 mg of Garfield nontronite suspended in 40 ml of 0.25 N CB buffer, then treated with varying amounts of $\text{Na}_2\text{S}_2\text{O}_4$ for 30 minutes at 70°C	14
Figure 2.1 The observed and predicted effects of ferrous iron composition on the surface charge, ω , of UPM, CZM, NZM, and GAN smectites. Pairs labeled either A or B represent separate sets of samples where the more oxidized member was initially reduced to the level of its more reduced companion with the same letter.....	21
Figure 3.1 Schematic drawing of the swelling pressure cell and adapter block, modified from the design used by Low (1980).....	28
Figure 3.2 The equilibrium water content, m_w/m_c , at various applied swelling pressures, Π , for smectites in various states of iron oxidation.....	32

Figure 3.3	The effect of iron oxidation state on the swelling pressure curves of Na^+ -smectites in 5×10^{-4} N NaCl solution.....	35
Figure 3.4	The relation between $\ln(\Pi+1)$ and m_c/m_w for the UPM, CZM, NZM, and GAN smectites in several different states of iron oxidation.....	37
Figure 3.5	The observed relation between Π and the surface charge, ω	39

Tables

Table 1.1	Clays used in this study, their unit-cell formulae, and natural compositions with respect to silicon, aluminum, and ferrous and total iron.....	4
Table 1.2	The effects of time, temperature and dithionite on the Fe^{2+} /total Fe ratio in CB buffered Garfield nontronite suspensions.....	13
Table 1.3	The release of Fe, Si, and Al from 100 mg of Garfield nontronite in 40 ml of 0.25 N CB buffer as affected by time, temperature, and $\text{Na}_2\text{S}_2\text{O}_4$	15
Table 2.1	The dissolution of Fe, Si, and Al during treatment with citrate-bicarbonate buffer (CB) and citrate-bicarbonate-dithionite (CBD).....	23
Table 2.2	The total quantities of Fe, Si, and Al dissolved from four smectites in 0.25 N citrate-bicarbonate buffer with (CBD) and without (CB) 200 mg of $\text{Na}_2\text{S}_2\text{O}_4$	24
Table 3.1	The ferrous iron content and corresponding mass ratios of water to clay, m_w/m_c , in equilibrium with various applied pressures, Π	31
Table 3.2	Correlation coefficients (r^2), and slopes (c), of m_w/m_c versus ferrous iron composition in the range 0-0.40 mmol Fe^{2+} /g clay.....	33
Table 3.3	The surface charge, ω , and swelling pressure, Π , of UPM, CZM, NZM, and GAN smectites in various states of reduction. The values for Π were obtained graphically from Fig. 3.3 at $m_w/m_c = 1.5$ g/g. The values for ω were obtained graphically from Fig. 2.1.....	34
Table 3.4	The estimated fraction of collapsed layers calculated from eq. [3-10] using DLVO theory to estimate λ . Units of Π are MPa.....	42

INTRODUCTION AND STATEMENT OF PROBLEM

The presence of swelling clays in soils and sediments is of great importance to many engineering, geologic, and agricultural problems. Dry clays swell to many times their original volume when they come into contact with water. If they are confined, they develop high swelling pressures that can disrupt pertinent structures and facilities. In cases where the swelling characteristics of an existing soil or sediment are detrimental to its intended use, it would be advantageous to have a method to modify its swelling properties in situ. The purpose of this study was to determine whether or not the swelling pressure of clay minerals is altered by changing the oxidation state of the iron in the clay crystal structure.

SUMMARY OF RESULTS

1. Methods, Techniques, and Apparatus

1.1. Introduction

Interest in the reduced (Fe^{2+}) form of iron-bearing smectites has increased markedly during recent years, but their characterization and use have been severely limited by the high susceptibility of reduced suspensions to reoxidation and by uncertainties surrounding the effects of reducing agents on the integrity of mineral structures (Rozenson and Heller-Kallai, 1976; Russell *et al.*, 1979). One problem with redox experiments with clays has been the presence of excess salts in the reduced product as the result of using sodium dithionite ($\text{Na}_2\text{S}_2\text{O}_4$) as the reducing agent. This largely precludes the quantitative analysis of reduced samples for Fe^{2+} and Fe^{3+} , the determination of surface charge, and the measurement of any other property such as water tension or swelling pressure that requires a low concentration of solutes in the solution external to the clay particles. Other reducing agents have been investigated, but dithionite is by far the most effective and the easiest to remove. However, conventional methods for removing excess salts require washing by either centrifugation, filtration, or dialysis. These processes commonly occur in the air with no provision for an inert atmosphere.

Another problem associated with reduced suspensions is that many measurements require a dried sample as either a powder or an oriented film, but the reduced state of the clay suspension changes readily upon drying if oxygen is present, even if excess dithionite remains. Oriented films prepared by drying from a suspension containing even modest levels of solutes are often brittle, and the solutes coat the surfaces rendering them unsatisfactory for most purposes.

Another area of concern has been the possible irreversible alteration of the mineral during reduction due to the dissolution of metals from the clay crystal structure. Russell *et al.* (1979) and Rozenson and Heller-Kallai (1976) observed that the Mossbauer spectrum of reduced-reoxidized nontronite has a much larger quadrupole splitting than does the spectrum of the unaltered material. Obviously, a drastic alteration occurred in the electronic environment of the iron. The effect of dithionite may, however, depend on other properties of the system such as the pH, the amount of tetrahedral iron present in the clay, and the presence of chelating agents. In the two studies mentioned above, the pH of the system was unbuffered and probably deviated markedly from neutral since $\text{Na}_2\text{S}_2\text{O}_4$ in H_2O forms an acid solution. The clay studied by Russell *et al.* (1979) contained a considerable amount of tetrahedral iron. Rozenson and Heller-Kallai (1976) studied the SWa-1 ferruginous smectite and reported that the originally yellow clay (oxidized) turned black upon reduction, then reoxidized to a rust color. They attribute this change to the release of up to 20% of the structural iron. Stucki and Roth (1977), on the other hand, observed a blue-green color for Garfield nontronite when reduced with dithionite

INTRODUCTION AND STATEMENT OF PROBLEM

The presence of swelling clays in soils and sediments is of great importance to many engineering, geologic, and agricultural problems. Dry clays swell to many times their original volume when they come into contact with water. If they are confined, they develop high swelling pressures that can disrupt pertinent structures and facilities. In cases where the swelling characteristics of an existing soil or sediment are detrimental to its intended use, it would be advantageous to have a method to modify its swelling properties in situ. The purpose of this study was to determine whether or not the swelling pressure of clay minerals is altered by changing the oxidation state of the iron in the clay crystal structure.

SUMMARY OF RESULTS

1. Methods, Techniques, and Apparatus

1.1. Introduction

Interest in the reduced (Fe^{2+}) form of iron-bearing smectites has increased markedly during recent years, but their characterization and use have been severely limited by the high susceptibility of reduced suspensions to reoxidation and by uncertainties surrounding the effects of reducing agents on the integrity of mineral structures (Rozenson and Heller-Kallai, 1976; Russell et al., 1979). One problem with redox experiments with clays has been the presence of excess salts in the reduced product as the result of using sodium dithionite ($\text{Na}_2\text{S}_2\text{O}_4$) as the reducing agent. This largely precludes the quantitative analysis of reduced samples for Fe^{2+} and Fe^{3+} , the determination of surface charge, and the measurement of any other property such as water tension or swelling pressure that requires a low concentration of solutes in the solution external to the clay particles. Other reducing agents have been investigated, but dithionite is by far the most effective and the easiest to remove. However, conventional methods for removing excess salts require washing by either centrifugation, filtration, or dialysis. These processes commonly occur in the air with no provision for an inert atmosphere.

Another problem associated with reduced suspensions is that many measurements require a dried sample as either a powder or an oriented film, but the reduced state of the clay suspension changes readily upon drying if oxygen is present, even if excess dithionite remains. Oriented films prepared by drying from a suspension containing even modest levels of solutes are often brittle, and the solutes coat the surfaces rendering them unsatisfactory for most purposes.

Another area of concern has been the possible irreversible alteration of the mineral during reduction due to the dissolution of metals from the clay crystal structure. Russell et al. (1979) and Rozenson and Heller-Kallai (1976) observed that the Mossbauer spectrum of reduced-reoxidized nontronite has a much larger quadrupole splitting than does the spectrum of the unaltered material. Obviously, a drastic alteration occurred in the electronic environment of the iron. The effect of dithionite may, however, depend on other properties of the system such as the pH, the amount of tetrahedral iron present in the clay, and the presence of chelating agents. In the two studies mentioned above, the pH of the system was unbuffered and probably deviated markedly from neutral since $\text{Na}_2\text{S}_2\text{O}_4$ in H_2O forms an acid solution. The clay studied by Russell et al. (1979) contained a considerable amount of tetrahedral iron. Rozenson and Heller-Kallai (1976) studied the SWa-1 ferruginous smectite and reported that the originally yellow clay (oxidized) turned black upon reduction, then reoxidized to a rust color. They attribute this change to the release of up to 20% of the structural iron. Stucki and Roth (1977), on the other hand, observed a blue-green color for Garfield nontronite when reduced with dithionite

in a near-neutral, citrate-bicarbonate medium. Upon reoxidation with either oxygen gas or H_2O_2 , the color returned to yellow. Other measurements also suggested that the process was largely reversible. None of these studies, however, included direct measurements of the amount of iron, aluminum and silicon released to the external solution during reduction. Techniques for handling reduced systems were too poorly developed to allow the quantitative analysis of the external solution.

Studies in our laboratories have focused on characterizing smectites in various states of oxidation, and have required measurements of swelling pressure; water content; surface charge; ferrous and ferric iron composition; magnetic susceptibility; and the x-ray diffraction, infrared, uv-visible, and Mossbauer spectra. An early realization was that conventional methods of sample preparation for these analyses were inadequate in preserving the reduced state, so special methods and apparatus were developed. Following is a description of these methods and apparatus, and illustrations of their use in addressing the problems outlined above.

1.2. Materials

The clays selected for this study, their unit-cell formulae, and their compositions with respect to silicon, aluminum, and ferrous and total iron are listed in Table 1.1. Each clay was Na^+ -saturated using a 1 N solution of NaCl, fractionated to $<2 \mu\text{m}$, dialyzed and freeze-dried.

The unit-cell formulae reported in Table 1.1 were calculated using the same weight percent values for Si, Al and Mg that were obtained in earlier studies (Low, 1980; Stucki et al., 1976); but the values for exchangeable Na^+ and ferrous and total iron were revised according to the results obtained from improved methods for ferrous and total iron analysis (Stucki and Anderson, 1981; Stucki, 1981).

1.3. Methods

Reduction of Clay Suspensions. A special reaction vessel was designed and constructed for the preparation of reduced suspensions. This vessel (Fig. 1.1) consisted of a 50 ml, round-bottom, polycarbonate centrifuge tube for which a special screw cap containing an imbedded septum was manufactured. The cap itself was made of aluminum with a 0.3 inch diameter hole drilled through the top. The resealable septum placed inside the cap consisted of two wafers 25 mm in diameter cut from a sheet stock (from LC Company) of silicone rubber bonded to teflon on one side with polyimide. The septum was supported by a PVC washer. A rubber gasket was placed between the washer and the rim of the tube to form an air-tight seal.

Using this reaction vessel, reduced clays were prepared by suspending 100-200 mg of freeze-dried clay in 10 ml of citrate-bicarbonate buffer solution, then diluting to 40 ml with purified water having a resistivity of 18 megohm/cm. The buffer solution was prepared by combining 8 parts of 1 N sodium bicarbonate (NaHCO_3) with 1 part of 0.3 M

Table 1.1. Clays used in this study, their unit-cell formulae, and natural compositions with respect to silicon, aluminum, and ferrous and total iron.

Smectite	Designation	Unit-cell Formula*	Based on Unit-cell Formula			
			Si	Al	Fe ²⁺	Total Fe
			-- -- mmol/g clay -- --			
Upton† Montmorillonite (API 25)	UPM	Na _{0.64} (Si _{7.82} Al _{0.18})(Al _{3.06} Mg _{0.65} Fe ³⁺ _{0.32})O ₂₀ (OH) ₄	10.518	4.358	0.015	0.539
Czechoslovakia #650 Montmorillonite†	CZM	Na _{0.48} (Si _{7.00} Al _{1.00})(Al _{2.63} Mg _{0.46} Fe ³⁺ _{1.17})O ₂₀ (OH) ₄	9.090	4.714	0.004	1.257
New Zealand† Montmorillonite	NZM	Na _{0.64} (Si _{7.32} Al _{0.68})(Al _{2.22} Mg _{0.51} Fe ³⁺ _{1.42})O ₂₀ (OH) ₄	9.407	3.724	0.007	1.502
Garfield Nontronite (API H-33a)	GAN	Na _{0.92} (Si _{7.12} Al _{0.88})(Al _{0.19} Mg _{0.11} Fe ³⁺ _{3.72} Fe ²⁺ _{0.01})O ₂₀ (OH) ₄	8.342	1.260	0.009	4.201 ¹ / ₄

*Corrected from Stucki et al. (1976) and Low (1980) using their values for Si, Al, and Mg, and the data from this study for Fe³⁺, Fe²⁺, and Na⁺.

†Described by Low (1980).

EXPLODED VIEW OF THE REACTION VESSEL

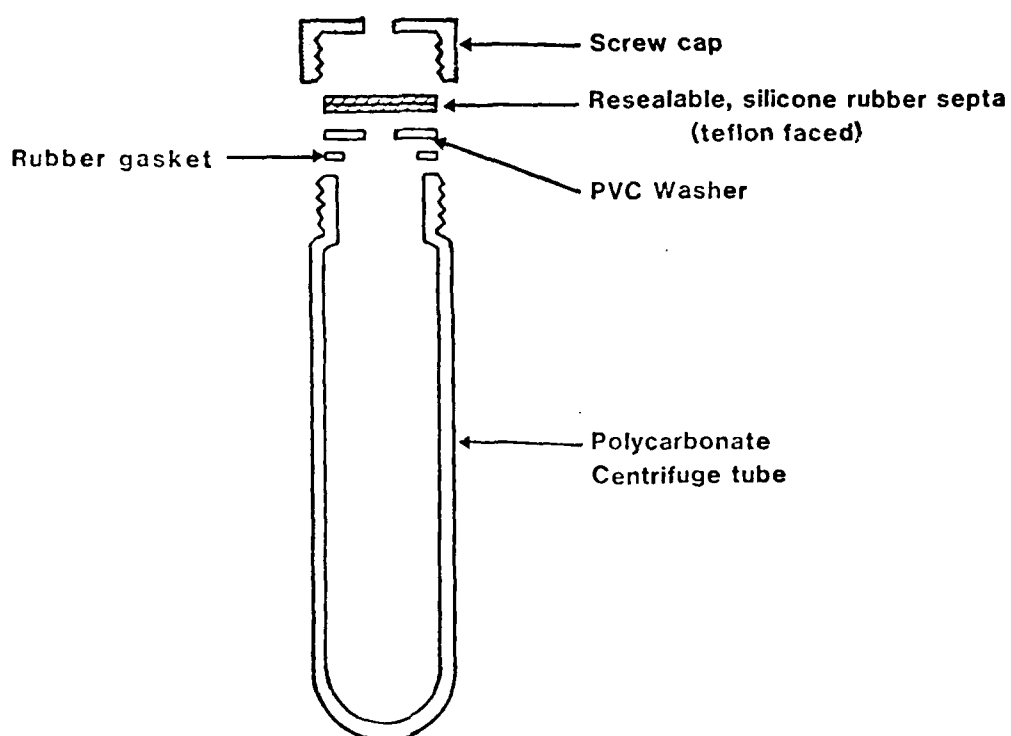


Figure 1.1 Schematic illustration of the reaction vessel used to prepare reduced smectite suspensions.

sodium citrate ($\text{Na}_3\text{C}_6\text{H}_5\text{O}_7 \cdot 2\text{H}_2\text{O}$). To the resulting suspension was added a portion of sodium dithionite ($\text{Na}_2\text{S}_2\text{O}_4$) salt ranging from 0 to 600 mg. Then the vessel was sealed and placed in a constant-temperature bath at either room temperature or 70°C for a specified length of time ranging from 5 minutes to 168 hours. The state of oxidation was determined using the method described by Stucki (1981) after removing the excess solutes from the sample.

Removal of Undesired Solutes. Undesired solutes were removed from the reduced suspensions by washing four times with a deoxygenated solution of $5 \times 10^{-3} \text{ N NaCl}$, followed by one wash with deoxygenated water (18 megohm/cm resistivity). Solutions were deoxygenated according to the following procedure, using the apparatus illustrated in Fig. 1.2. The solution to be deoxygenated was siphoned into the flask through the condensor by applying vacuum to the suction port; or, alternatively, it was added through the neck of the flask with the condensor removed. Oxygen-free nitrogen gas was then passed through the solution via a gas dispersion tube and the solution was boiled vigorously with stirring for about one hour. To prevent pressure build-up in the flask, the stopcock was opened and a steady flow of nitrogen was maintained across the top of the condensor column. After the solution had cooled, the stopcock was closed and the flow of nitrogen removed. Portions of the solution were then removed as needed through the solution outlet port. Safety shields were placed around the deoxygenating units in case of accidental excess pressurization of the system.

Clay suspensions were washed by centrifuging (IEC Model B-20A centrifuge, slant head no. 870) with a force of about $35,000 \times g$, and exchanging the supernatant with the desired wash solution using the apparatus illustrated in Fig. 1.3. Access to the tube contents without opening the reaction vessel was achieved using 6-inch, 22 gauge, septum penetration needles made on special order by Popper & Sons. The tip of these needles was designed with the orifice in the side wall rather than in the bevelled end of the needle, thus allowing the needle to penetrate the septum without coring a hole. Two needles were inserted into the reaction vessel, and two into the collection flask. By proper positioning of valves 1, 2, and 3 the collection flask was evacuated and the reaction vessel was pressurized with oxygen-free nitrogen gas. The decanting needle, connected to the flexible tubing leading to the collection flask, was lowered into the clear supernatant solution of the sample to a point just above the sediment in the bottom, and the supernatant was decanted in response to the pressure gradient. The liquid volume in the reaction vessel was replaced with nitrogen gas. When the supernatant transfer was completed, the decanting needle was raised, and valve 2 was adjusted to connect the sample to the desired deoxygenated solution, i.e., either H_2O or $5 \times 10^{-3} \text{ N NaCl}$. Valve 2 was positioned so that the atmosphere above the solution selected by valve 1 was pressurized (~ 35 psig) with nitrogen. This facilitated the transfer of fresh solution to the sample and helped maintain the integrity of the deoxygenated liquid.

DEOXYGENATING UNIT

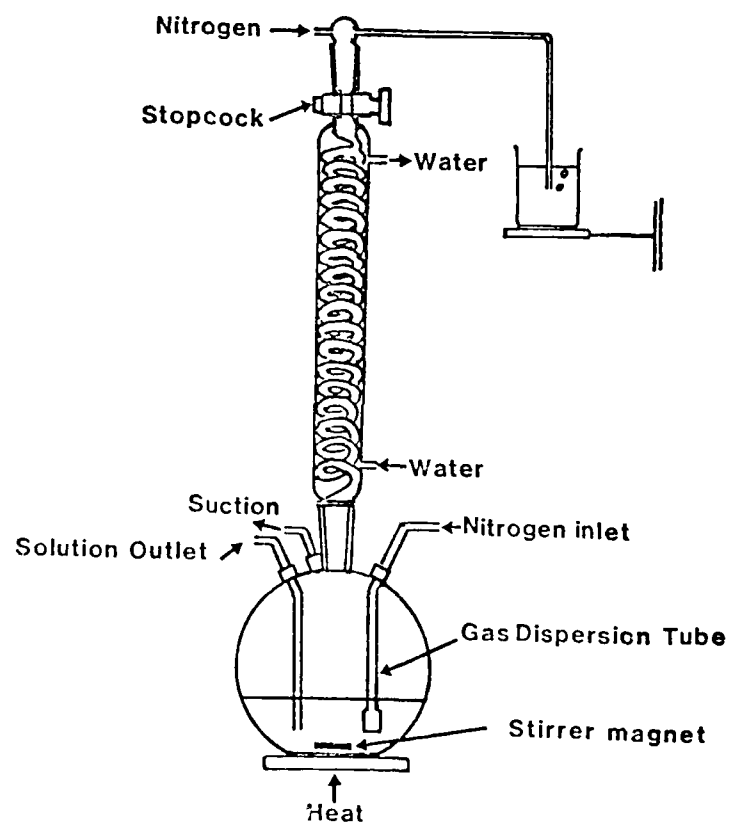


Figure 1.2 Schematic drawing of the glass apparatus for deoxygenating solutions.

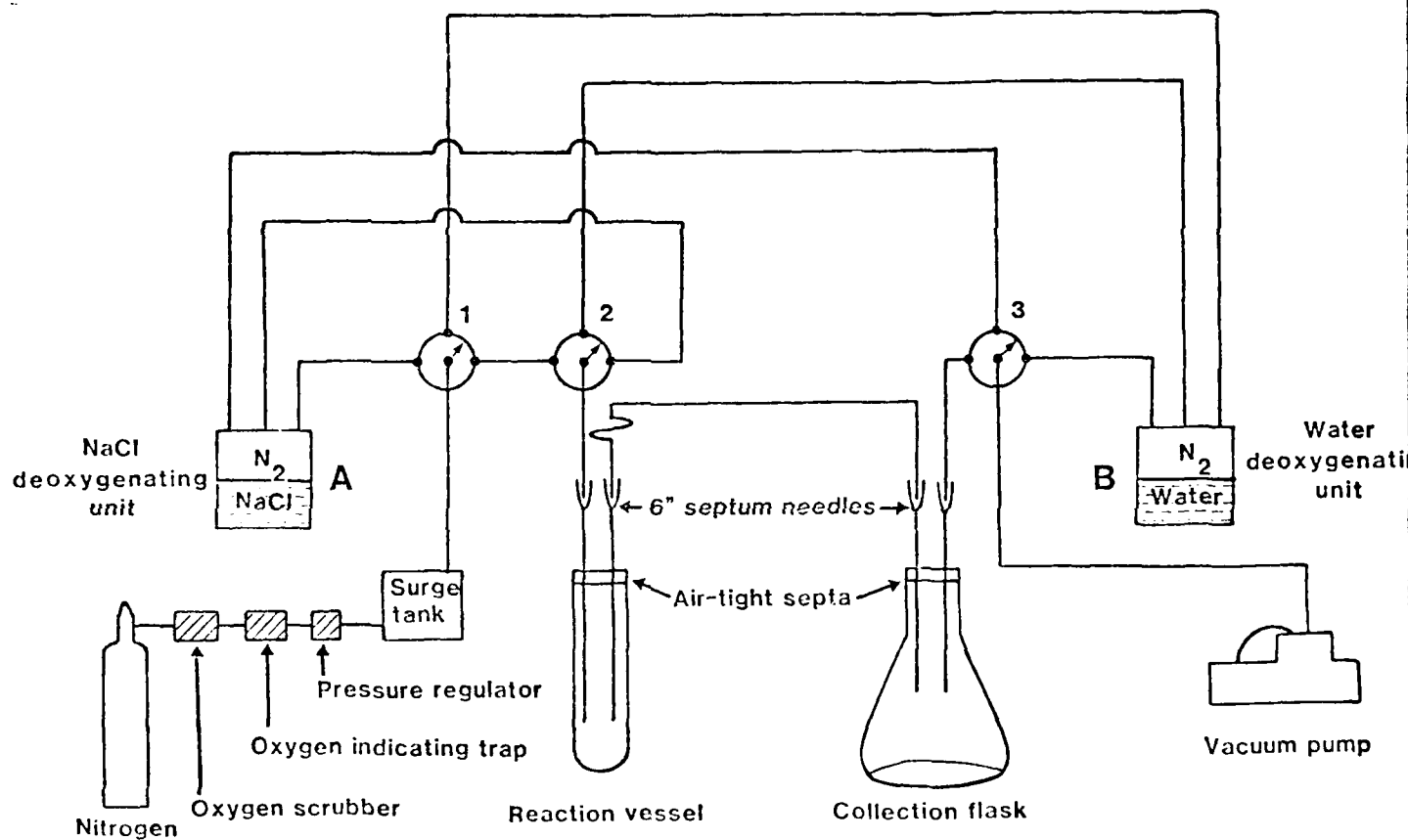


Figure 1.3 Schematic drawing of the apparatus for exchanging and collecting supernatant solutions under an inert atmosphere. (For a more detailed view of the deoxygenating units see Fig. 1.2).

When the reaction vessel was filled with about 40 ml of fresh wash solution, it was removed from the apparatus and the clay sediment was resuspended using a vortex mixer. The more stubborn sediments (as a result of longer centrifugation times) were resuspended by placing the vessel directly on the vortex mixer immediately as fresh solution began to enter. Sediments from the highest centrifugation times (ca. 30-60 minutes) required, in addition, a short (30-60 second) sonic treatment with a 3-inch cup horn (Branson Model 314-012-020) filled with water. Using 5×10^{-3} N NaCl as the wash solution, four washing cycles were sufficient to reduce the sodium concentration in the clay to that of the wash solution. Further dilution was achieved, when desired, by resuspending the clay in deoxygenated water after the final wash. Typically, this dilution was by a factor of 1:10.

The principal limitations of this method of dialysis are: 1) a maximum of about 500 mg of clay can be treated in a single reaction vessel due to the volume capacity of the vessel and to the possibility of gel formation when the mass ratio of clay to water exceeds 10 mg/g; 2) the reaction vessel must be made of clear material to allow the operator to visually follow the insertion of the decanting needle into the supernatant solution so as much solution as possible can be decanted without disturbing the sediment in the bottom of the vessel; and 3) the reaction vessel is designed to withstand a maximum force of 40,000 x g, which is insufficient to produce a clear supernatant upon centrifugation when clay-size particles less than $0.02 \mu\text{m}$ (e.s.d.) are present. Since none of the supernatants of the clays used in these experiments were clear after centrifuging for 60 minutes at 35,000 x g, it was necessary to add a minimum amount of NaCl (5×10^{-3} N) to the wash solution.

Valves 1, 2, and 3 of the apparatus in Fig. 1.3 were brass, multi-port ball valves manufactured by the Whitey Co., Highland Heights, OH. The various components of the apparatus were connected with 1/8 inch (od) polyethylene tubing, except the needles which were connected by leur-lock fittings.

Assay of Solutions for Fe, Al, Si, and Na. Using the decanting apparatus (Fig. 1.3), the supernatant solution from each washing was collected into a separate 50 ml PMP erlenmeyer flask with a threaded top. The contents of each flask were subsequently analyzed for Si using the vanado-molybdate method described by Weaver et al. (1968), and for Al and Fe by atomic absorption spectrometry. Al was determined in a nitrous oxide-acetylene flame at 309.3 nm, and Fe in air-acetylene at 248.3 nm using a Perkin-Elmer Model 5000 spectrometer. Total Fe was also determined colorimetrically using the method of Stucki (1981) after oxidizing the dithionite with air. The extent of dissolution of these elements from the clay was evaluated by summing the amounts detected in all solutions collected from each sample. The concentrations of Na in the final supernatant solution were determined for selected samples by atomic emission spectrometry at 589 nm.

Reoxidation. Following the third wash with 5×10^{-3} N NaCl, samples to be reoxidized were uncapped and O_2 gas was passed through the clay suspension using a 6-inch needle. The oxygen flow rate was adjusted to prevent sample loss, and evaporation of the suspension was minimized by first passing the gas through a water bath using a side-arm flask and gas dispersion tube. Thirty minutes of reoxidation in this manner was sufficient to produce extensive, although incomplete, reoxidation. Some clays were reoxidized for as long as 24 hours to increase reoxidation.

Preparation of Dry Films. Clay suspensions were dried in the apparatus illustrated in Fig. 1.4. It consists of a $1 \times 2 \times 1/4$ inch ceramic plate (15 bar) imbedded in a depression of slightly larger size in the top of a no. 13 rubber stopper housed inside a cylindrical plexiglas chamber. An aluminum bracket with an underlying rubber gasket was clamped onto the top of the ceramic plate with two bolts that penetrated the rubber stopper and the bottom bulkhead of the chamber. When tightly clamped, this bracket formed an air-tight seal around the top edges of the ceramic plate, and the compression on the rubber stopper sealed the bottom of the chamber. A drain to the underside of the ceramic plate was formed by drilling a hole vertically through the center of the stopper and the bottom of the chamber, then a glass tube was inserted into the stopper from the bottom and a short extension of tygon tubing was added to the free end of the glass tube. The top of the chamber was threaded onto a brass adaptor block connected to a ball valve on the top and a source of inert gas on one side pressurized to about 0.35 MPa.

Oriented films for x-ray diffraction were prepared from washed suspensions by first purging the cell for two minutes with oxygen-free nitrogen gas, then about 3 ml of clay suspension was delivered through the open ball valve onto the ceramic filter using an air-tight syringe with a 6-inch long needle. The wall of the aluminum bracket is 0.125 inches thick, rising vertically from the top of the ceramic plate, and thus forms the walls of a small reservoir to hold the clay suspension during filtration. The ball valve was then closed and the system became immediately pressurized. Once the excess water had drained from the clay, the supply pressure was reduced and, since the side walls of the ceramic plate were not sealed, the nitrogen was able to continue flowing in a very slow stream to complete the drying of the sample by evaporation. Once completely dry, the ceramic plate with sample intact was transferred directly to the x-ray diffractometer.

Self-supporting films were prepared in a similar manner except a membrane filter (0.025 μ m pore size) was placed between the clay suspension and the surface of the ceramic plate. Due to the very small pore size of the membrane filter, most clays will not penetrate it and thus can be removed easily as a self-supporting film. In cases where the clays did adhere to the membrane filter, a mylar sheet was substituted by stretching it across the ceramic plate and drying the sample by evaporation into the slow stream of nitrogen flowing through the system.

PRESSURE CELL FOR PREPARATION OF XRD-SLIDES
AND SELF SUPPORTING CLAY FILMS, UNDER OXYGEN FREE CONDITIONS

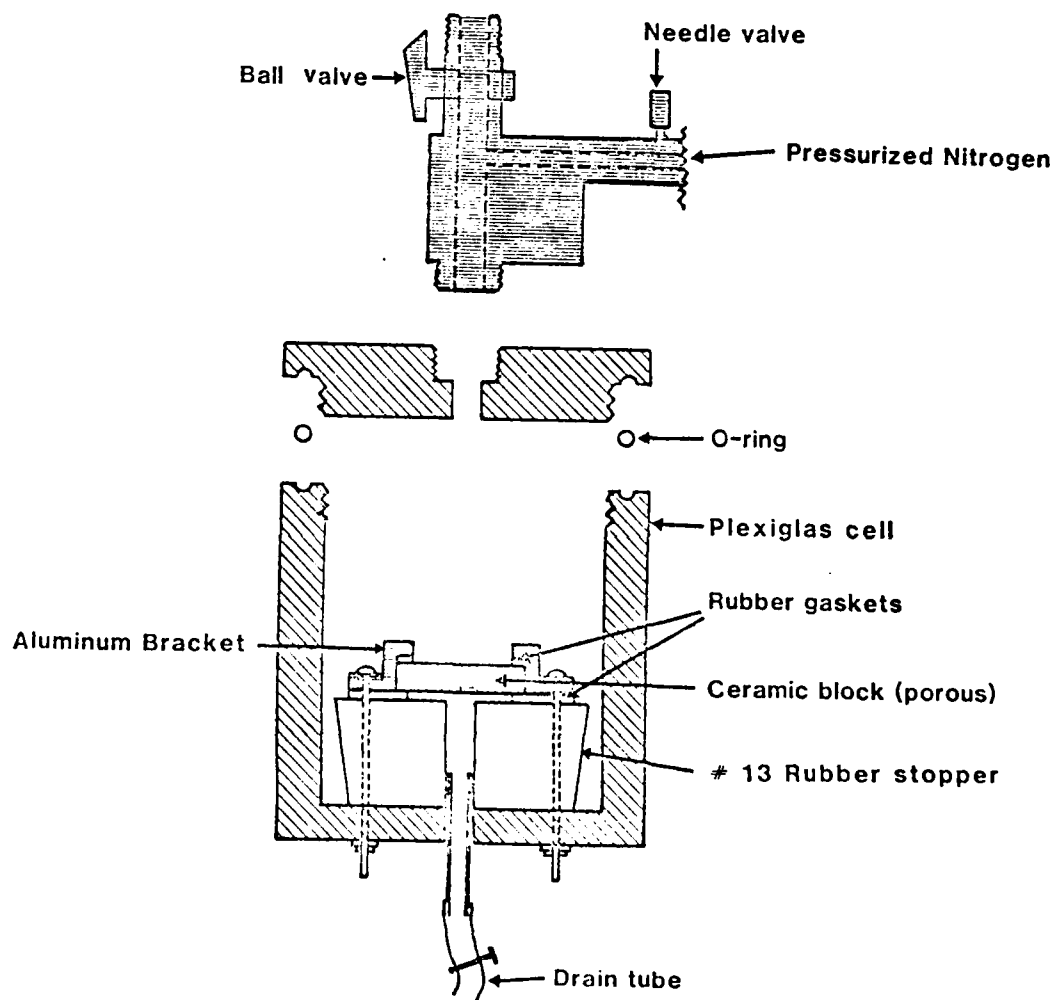


Figure 1.4 Schematic drawing of the chamber used to prepare oriented films of reduced smectites.

Dry, powdered samples were prepared by freeze-drying in a nitrogen atmosphere.

1.4. Results

The procedures and apparatus described above were very effective in decreasing the solute concentration in the clay suspension while maintaining a high level of reduction. This is illustrated by comparing the $\text{Fe}^{2+}/\text{total Fe}$ ratios of three identical samples of Garfield nontronite reduced for 15 minutes at 70°C using 200 mg of dithionite to 100 mg of clay in a CB buffered medium: one sample was washed four times with the deoxygenated, $5 \times 10^{-3} \text{ N}$ NaCl solution as described in the procedure; the second was washed similarly except at one point in the procedure the cap was removed from the reaction vessel momentarily to expose the contents to atmospheric oxygen; and the third was washed four times with the same NaCl solution but prior to its deoxygenation, and the cap was removed each time to exchange solutions. The respective ratios of $\text{Fe}^{2+}/\text{total Fe}$, were 0.343, 0.324, and 0.026. During one trial, the sample washed with non-deoxygenated solutions was otherwise kept under an inert atmosphere by using the decanting apparatus to exchange supernatant solutions rather than removing the cap from the reaction vessel. The extent of reoxidation was significantly less than when the cap was removed. Clearly, the method and apparatus described above yield a much more reduced product than conventional techniques, and are superior to those used by Stucki and Roth (1977) who reported much greater reoxidation after one brief exposure to the atmosphere. Oxygen in the air space above the reduced suspension appears to have a greater influence on reoxidation than does the oxygen dissolved in the wash solution. Obviously this is the result of the relative amounts of O_2 in these respective phases and depends on the volume of the air space. One cannot conclude with certainty, however, that these techniques prevent reoxidation completely. This would require the quantitative measure of Fe^{2+} and total Fe directly in the reduced, unwashed suspension. The only method we are aware of that potentially could do this is Mossbauer spectroscopy, and we have thus far been unable to perform the necessary analyses by that technique.

The concentration of Na^+ in the supernatants from the four washings of these samples was determined by atomic emission to be $5.02 \times 10^{-3} \text{ mol/L}$. This corresponds to the initial concentration of the wash solution and indicates that the washing is complete after four cycles.

The level of reduction that can be achieved in any given sample depends on a number of factors, including: the concentration of dithionite in the suspension, the mass ratio of dithionite to clay (D_c), the reaction time, and the temperature. In Table 1.2 are summarized the $\text{Fe}^{2+}/\text{total Fe}$ ratios measured in Garfield nontronite following treatments in which all of these factors were varied systematically. The values for Fe^{2+} and total Fe were determined on the wet gel remaining after the fourth washing cycle. At room temperature the rate of reduction is relatively slow, and the reduction ratio exceeded 0.5 only after about 168 hours of reaction time. A six-fold increase in D_c

increased the initial rate of the reaction almost nine-fold, but produced only about a 20% increase in the overall reduction ratio after 168 hours.

Table 1.2. The effects of time, temperature and dithionite on the ratio of Fe^{2+} /total Fe in CB buffered Garfield nontronite suspensions.

Sample No.	mg Clay	mg Dithionite Added	time, hr.	Fe^{2+} /Total FE
-----25°C-----				
1	100	200	0.25	.008
2	100	200	168.0	.514
3	200	200	0.083	.008
4	100	600	0.25	.073
5	100	600	168.0	.611
-----70°C-----				
6	100	200	0.25	.326
7	100	200	168.0	.702
8	200	200	0.50	.472
9	200	200	0.083	.038
10	200	200	0.50	.306
11	200	200	1.00	.360
12	200	200	3.00	.477
13	100	600	0.25	.554
14	100	600	168.0	.779

The rate of reduction increased markedly by raising the temperature to 70°C, but apparently had only a modest effect on the ultimate, attainable ferrous iron composition of the clay. Even with the increased initial rate, reaction times of several hours were still required for the reduction ratio to exceed 0.5, and the maximum ratio observed in Garfield nontronite is on the order of 0.80. This does not necessarily infer, however, that greater reduction is impossible or did not occur in the unwashed suspensions at either temperature.

The ferrous iron composition was varied from one sample to another either by adjusting the amount of dithionite added to the suspension, and thus altering the initial level of reduction; or, by reducing all samples under identical conditions, then reoxidizing to different points by passing H_2O -saturated oxygen gas through the reduced

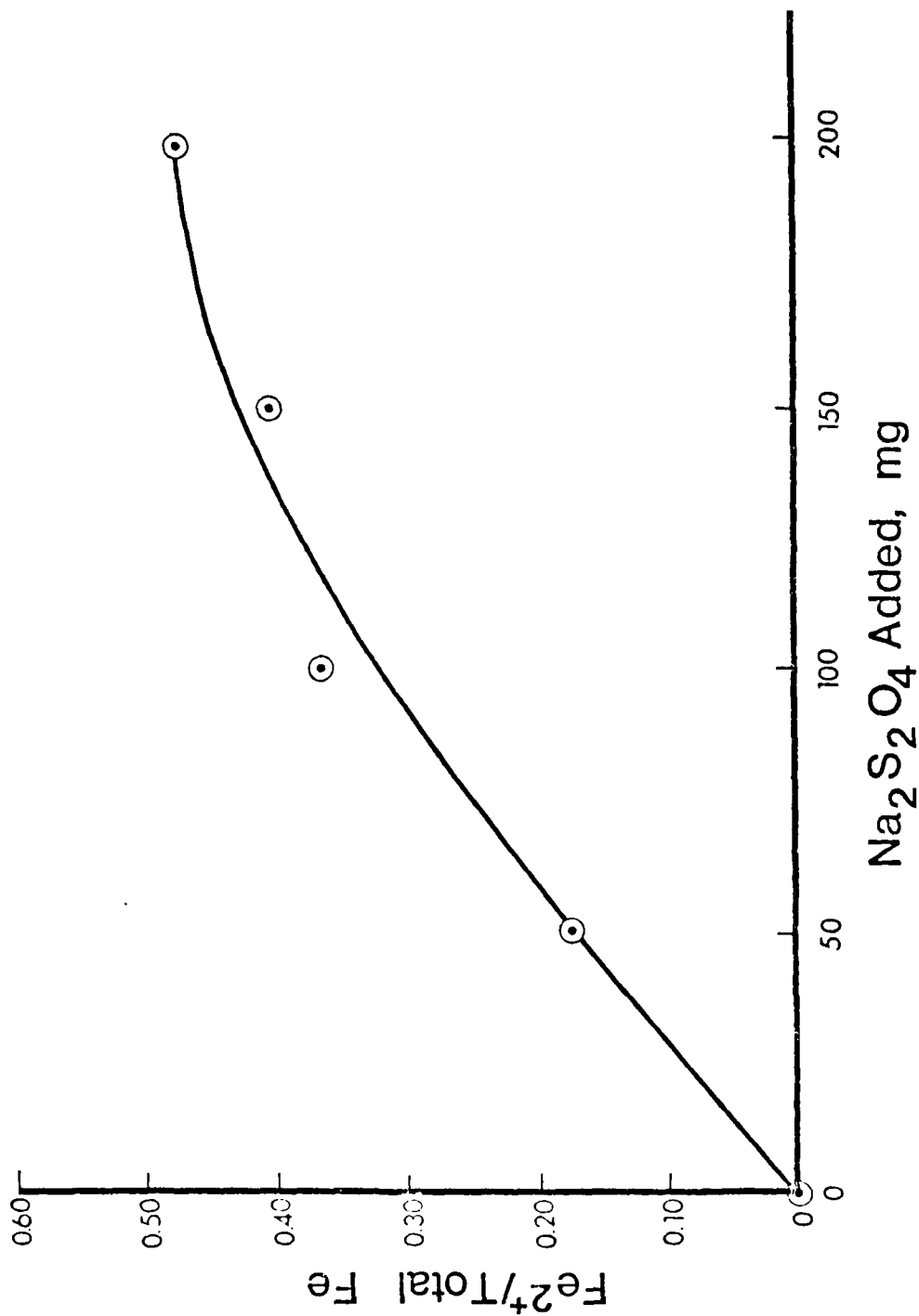


Figure 1.5 $\text{Fe}^{2+}/\text{total Fe}$ ratios for 100 mg of Garfield nontronite suspended in 40 ml of 0.25 N CB buffer, then treated with varying amounts of $\text{Na}_2\text{S}_2\text{O}_4$ for 30 minutes at 70°C .

suspensions for different lengths of time. The effect of varying the amount of dithionite is illustrated in Fig. 1.5, and shows a general trend toward increased ferrous iron content. These relationships should be regarded as qualitative rather than as quantitative because the curves could shift depending on possible variations in the air volume above the suspension, the efficiency of the oxygen traps, the purity of the nitrogen gas, or the seal of the reaction vessel cap.

Treatment of the clay with dithionite in 0.25 N CB buffer caused iron, silicon, and aluminum to appear in the solution external to the clay crystals (Table 1.3). The amount of element released depended on the time of exposure to the CBD medium, the temperature, and the amount of dithionite added relative to the amount of clay. The total amount of iron and silicon released was very small, though it did increase gradually as the condition variables increased. But even after the more severe treatments with dithionite, only 2-3% of the total iron was dissolved. This is much below the value of 20% reported by Rozenson and Heller-Kallai (1976), and indicates that the reducing conditions greatly affect the extent of dissolution of iron. Further, the Fe/Si ratios in solution indicate a slight tendency for the dissolution to become more selective for iron as the amount of dithionite increases, but the range varies from less than half to about twice the elemental mass ratio derived from the structural formula.

Table 1.3. The release of Fe, Si, and Al from 100 mg of Garfield nontronite in 40 ml of 0.25 N CB buffer as affected by time, temperature, and $\text{Na}_2\text{S}_2\text{O}_4$.

Treatment				Amount of Element Released				
Time	Temp	$\text{Na}_2\text{S}_2\text{O}_4$	$\text{Fe}^{2+}/$ Total Fe	As % of Total Element			As Mass Ratio* to Si Released	
hr	°C	mg		Fe	Si	Al	Fe	Al
0.25	25	0	0.003	0.15	0.42	8.38	0.38	2.87
0.25	25	200	0.008	0.63	0.63	8.28	1.07	1.91
0.25	25	600	0.073	1.69	0.81	10.15	2.23	1.82
0.25	70	200	0.326	1.84	1.39	4.81	1.41	0.50
0.25	70	600	0.554	2.08	0.80	4.55	2.80	0.83
168	25	0	0.004	0.14	0.50	7.77	0.28	2.10
168	25	200	0.514	2.42	1.80	4.49	1.44	0.36
168	25	600	0.611	3.89	3.17	6.04	1.31	0.28
168	70	20	0.702	1.69	3.34	2.99	0.54	0.13
168	70	600	0.779	2.72	7.80	5.39	0.37	0.10

*Based on the unit-cell formula of Garfield nontronite (Stucki *et al.*, 1976), the mass ratios in the structure are: $\text{Fe/Si} = 1.068$; $\text{Al/Si} = 0.145$.

The dissolution of aluminum was much more extensive than Fe or Si, and the highest level was observed in the treatment that had citrate and bicarbonate but no dithionite. The loss of Al is thus the result of reaction with citrate-bicarbonate rather than with dithionite or as the result of iron reduction. Comparing Fe/Si and Al/Si ratios, one finds that the Fe/Si ratios in solution roughly follow the structural ratio, whereas Al/Si ratios are an order of magnitude greater than the ratio in the mineral. One must, therefore, conclude that Al is selectively dissolved from the mineral. About 4% of the clay mass is aluminum, which occupies about 9% of all the cationic sites in the crystal structure. By losing 8% of the Al, only 0.32% of the total mass and a maximum of 0.72% of all the occupied cationic sites have been affected by this dissolution. The effects of CB and CBD treatments on the dissolution of clays will be discussed at greater length in section 2.

1.5. Conclusions

Studies designed to characterize and use clays in their reduced state require methods that guard against air oxidation. The methods and apparatus described in this report were effective in removing excess undesired solutes from reduced smectite suspensions while maintaining a high level of ferrous iron composition. They also enabled the preparation of dried, reduced films preferentially oriented with respect to the crystallographic c-axis for analysis by x-ray diffraction and infrared spectroscopy. Supernatant solutions were collected and analyzed for iron, aluminum, and silicon, from which the extent of dissolution of the clay as a result of CBD treatment was assessed. Results indicated that very little iron and silicon were dissolved, but as much as about 8% of the total aluminum was removed by the citrate-bicarbonate buffer solution.

2. The Effect of CBD Treatment and of Reoxidation on Surface Charge and Dissolution.

2.1. Introduction

When ferric iron in the octahedral sheet of a clay mineral is reduced to ferrous, the negative surface charge of the clay should increase linearly with respect to the concentration of Fe^{2+} in the structure. This predicted relationship has important consequences relevant to the macroscopic properties of the mineral. According to DLVO theory, the swelling of clay in water is largely osmotic and should increase with surface charge density (Verwey and Overbeek, 1948). Low and co-workers (Odom and Low, 1978; Low and Margheim, 1979; Low, 1980, 1981), on the other hand, have demonstrated that swelling of smectites is largely independent of surface charge, asserting that surface area is the determining factor. A knowledge of the precise effects of iron oxidation state on surface charge would be very useful in evaluating these apparently conflicting theories of clay swelling. Also, increasing the layer charge of a smectite mineral may cause its layers to collapse like a vermiculite or glauconite, and thus dramatically alter the surface area and other mineral properties. These alterations could have important practical applications and could provide more complete information about the mechanisms for mineral weathering and the oxidation and reduction of iron in clay minerals.

Experimental verification of the effect of iron oxidation state on surface charge is difficult because conventional methods for determining cation exchange capacity (CEC) require numerous washings that can cause reoxidation. For example, Roth *et al.* (1968) reported that the CEC of Garfield nontronite remained constant with the reduction of structural iron. But after careful examination of their procedure, it is evident that no precautions were taken to prevent reoxidation. When reduced suspensions of the same clay were washed with degassed solution, using serum stoppers to isolate the samples from the atmosphere, Stucki and Roth (1977) observed a reversible increase in CEC.

Another difficulty is the possible readsorption of iron, silicon, or aluminum dissolved from the mineral structure during chemical reduction. These ions could block some cation exchange sites and render the CEC an inaccurate measure of the layer charge. Clays containing tetrahedral iron are particularly susceptible to irreversible alteration when reduced with dithionite (Russell *et al.*, 1979), but even clays with very little tetrahedral iron, such as Garfield nontronite, can suffer some dissolution (See Section 1 above). It appears, however, that dissolution of clays containing little or no tetrahedral iron is minimized when the pH is maintained near neutral, as evidenced by the reversibility of the CEC in Garfield nontronite.

Stucki and Roth (1977) reported only three reduction ratios for a single clay, Garfield nontronite, which was sufficient to illustrate an increased CEC upon iron reduction, but does not address the question of whether this phenomenon occurs generally in other smectites. The

purpose of this study was to establish a more complete understanding of the relationship between iron oxidation state and surface charge by studying several different clays over a wide range of Fe^{2+} /total Fe ratios, and to evaluate the possible effects of clay dissolution on surface charge determinations.

2.2. Methods and Materials

Using the methods and apparatus described in Section 1, 200 mg of clay was added to a preweighed reaction vessel (Fig. 1.1), suspended in 40 ml of 0.25 N citrate-bicarbonate (CB) buffer, and reduced with 200 mg of $\text{Na}_2\text{S}_2\text{O}_4$ at 70 C for 30 minutes. The sample was washed four times with a deoxygenated solution of 5×10^{-3} N NaCl. Supernatants were saved in 50 ml PMP erlenmeyer flasks, then analyzed for Fe, Si, and Al. The supernatant from the fourth wash was also assayed for Na.

After decanting the final supernatant, the vessel was weighed again to determine the weight of the entrained solution, then the clay was redispersed in 10 ml of deoxygenated H_2O (18 megohm/cm resistivity). One 2 ml portion of the suspension was transferred to a pressure cell under an inert atmosphere using an air-tight syringe, and most of the water was extruded from the clay through a porous, membrane filter at the base of the cell. The resulting gel was transferred to a 100 ml polypropylene centrifuge tube and analyzed immediately for Fe^{2+} and total Fe using the method described by Stucki (1981). The remainder of the suspension was frozen with liquid nitrogen and lyophilized. Then an accurately weighed portion (~10 mg) of the resulting freeze-dried material was digested in a 100 ml polypropylene centrifuge tube (Stucki, 1981). An aliquot from the diluted digestate was transferred from the digestion tube to a 50 ml PMP erlenmeyer flask and diluted 1:10 with H_2O using an automatic dilutor, and the concentration of Na^+ in this solution was determined by flame emission on a Perkin-Elmer Model 5000 spectrophotometer at 589 nm in an air-acetylene flame. A set of sodium standards ranging from 0-0.174 mmol/L were prepared by taking selected aliquots of a standard NaCl solution through the identical procedure. The standard curve was linear up to 0.087 mmol/L, and with the dilution ratios used all samples analyzed were well within the linear range. The supernatant solution saved from the fourth washing was analyzed for Na^+ in like manner after diluting 1:100 into a 50 ml PMP erlenmeyer flask. A separate set of standard solutions was prepared to simulate the matrix solution of the supernatant.

The method for calculating surface charge from these measurements was based on the total Na^+ in the digested sample, and corrected for the portion attributable to Na^+ in the external solution. This required correction terms in the mass of the freeze-dried gel, and in the amount of total Na^+ observed in the digested portion of the sample. The total mmols of Na^+ , N_s , in the entrained solution of the gel is given by

$$N_s = c_s f_s V_{es} \quad [2.1]$$

where

c_s = concentration of Na^+ in the diluted supernatant solution, mmol/L.

f_s = dilution factor for the supernatant solution, ≈ 10

V_{es} = volume of supernatant entrained in the clay gel prior to freeze-drying, L.

If c_s is non-zero, then the total mass of the freeze-dried gel, w_t , will consist of two parts: the Na^+ -saturated clay, and the NaCl from the external solution. The portion of w_t attributable to the clay is then given by

$$w_c = w_t - 0.0584 c_s f_s V_{es} \quad [2.2]$$

where the numerical coefficient converts the units of the second term on the right from mmole to g. The clay fraction of the dried gel, then, is

$$x_c = \frac{w_t - 0.0584 c_s f_s V_{es}}{w_t} = \frac{w_c}{w_t} \quad [2.3]$$

The NaCl fraction is

$$x_n = \frac{0.0584 c_s f_s V_{es}}{w_t} = \frac{w_t - w_c}{w_t} \quad [2.4]$$

The mass of clay digested, m_c , and the amount of excess NaCl in the digestate, m_n , are then obtained from the relations

$$m_c = m_t x_c \quad [2.5]$$

and

$$m_n = m_t x_n \quad [2.6]$$

where m_t is the mass of dried gel transferred to the digestion tube. The expression for calculating the surface charge, ω , is

$$\omega = \frac{V_t c_d f_d - 17.11 m_n}{m_c} \quad [2.7]$$

where

V_t = volume of the diluted digestate, ≈ 0.080 L.

c_d = concentration of Na^+ in the final dilution of the digestate solution, mmol/L.

f_d = dilution factor for the final dilution of the digestate solution, ≈ 10

The numerical coefficient simply converts units from g back to mmole. After substituting for m_n and m_c , equation [2.7] can also be expressed in terms of the measured variables, viz.

$$\omega = \frac{w_t V_t c_d f_d - c_s f_s V_{es} m_t}{m_t (w_t - 0.0584 c_s f_s V_{es})} \quad [2.8]$$

This method assumes that the layer charge is neutralized completely and solely by Na^+ .

Variations in the reduction ratios were achieved either by reoxidizing a reduced sample, or by varying the amount of $Na_2S_2O_4$ added (See Section 1 for details). The layer charge of the original clay was determined by submitting the sample to the same treatment as the reduced samples, except the dithionite was omitted.

2.3. Results and Discussion

Results showing the effect of iron oxidation state on the surface charge of UPM, CZM, NZM, and GAN are presented in Fig. 2.1. The plotted values were obtained from clays in CB buffer (pH=8) that were unreduced, reduced to various reduction ratios, or reduced then reoxidized. For each of the four clays studied, the reduction of Fe^{3+} to Fe^{2+} in the octahedral sheet increased the surface charge of the clay. In the range of 0 to ~ 0.3 mmol Fe^{2+} /g clay, the surface charge increased according to linear relationships obtained from charge deficit calculations (Gast, 1977), assuming only that the relative proportions of Fe^{3+} and Fe^{2+} in the octahedral sheet were altered but the total composition was otherwise constant. Above this range, deviations from the predicted lines were observed for all four clays and an apparent maximum value was observed for each clay. In the case of GAN, where the attainable level of reduction is not as limited, the surface charge actually decreased after reaching a maximum.

To determine the reversibility of the response of surface charge to iron reduction treatments, the history of a reoxidized sample was traced by preparing a set of two samples reduced under identical conditions. One sample was reoxidized by passing H_2O -saturated oxygen gas through the partially washed suspension, then the surface charge and reduction ratio were determined in each sample. This was repeated for two sets of samples in both the GAN and UPM clays. These values were then superimposed on the plots (Fig. 2.1) of surface charge versus ferrous iron composition of other samples of the same clays where the different reduction levels were achieved by varying the amount of reducing agent. The sets of reduced and reoxidized pairs are identified in Fig. 2.1 by the arrows labelled with the letters A and B. The points for the reoxidized samples fall very close to the lines connecting the points obtained by reduction, regardless of the level of reduction to which the sample was first taken. Thus, at one point in time the characteristics of the reoxidized sample were identical to the characteristics of its more reduced companion. Following oxidation with oxygen, these characteristics were altered to closely resemble

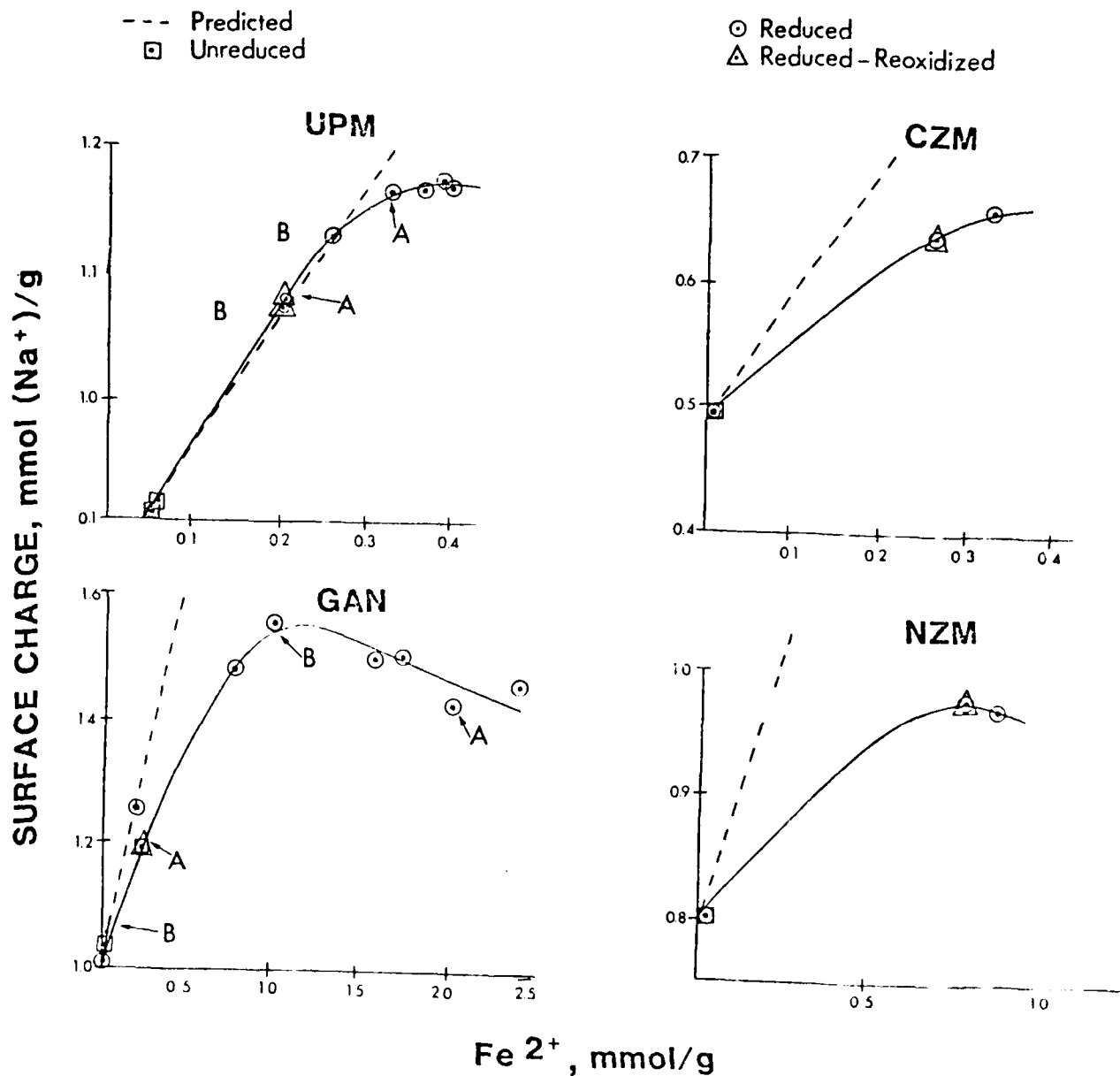
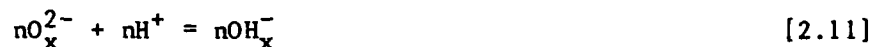
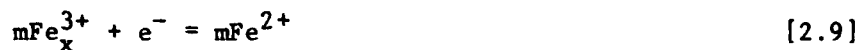


Figure 2.1 The observed and predicted effects of ferrous iron composition on the surface charge, ω , of UPM, CZM, NZM, and GAN smectites. Pairs labelled either A or B represent separate sets of samples where the more oxidized member was initially reduced to the level of its more reduced companion with the same letter.

those of samples that had reached that state of oxidation by the alternate path of reduction without reoxidation. In other words, the process is reversible within a few mmol Na⁺/g clay.

Since the observed charge deviates from the predicted values, other changes in the mineral composition are required. The net effect of any such change must be to balance the increased negative charge due to Fe³⁺ reduction. Stucki and Roth (1977) proposed that structural hydroxyls are lost during reduction, and a modified version of their proposed mechanism is



where m and n are stoichiometry coefficients, * indicates the proton initially present as part of the structural hydroxyl ion, and x denotes the species in the clay structure. Other alterations in mineral composition are discussed below, and could offer alternative explanations for the observed deviations in surface charge. But the mechanism of Stucki and Roth (1977) at this point seems quite reasonable.

Measurable quantities of Fe, Si, and Al were released from the clay into the supernatant solution during CBD treatment and subsequent NaCl washings. The CB buffer without dithionite also invoked some dissolution. Most of the dissolved Fe and Si was recovered in the initial extract (Table 2.1), diminishing sharply in subsequent washings. The total quantities recovered were greater from the CBD than from the CB solutions, but amounted to only a small fraction (0.4-4 percent) of the total iron and silicon initially present in the mineral (Table 2.2). This translates into the loss of only a fraction of a percent of the clay mass, except for the CZM clay where the amount of iron and silicon recovered in solution summed to about two percent of the original clay weight. The higher mole ratios of Fe/Si in solution, as compared to the unit-cell mole ratios (Table 2.2), indicate that dissolution is moderately selective for Fe relative to Si. The selectivity for Fe was stronger in CZM than in the other clays.

The increased dissolution of iron and silicon following treatment with the reducing agent most likely is the result of Fe²⁺ formation in the clay structure rather than acid dissolution since the pH stays near or above neutral. The replacement of Fe³⁺ with Fe²⁺ could create local instabilities in the crystal field energies of the iron sites and thus provide the basis for structural rearrangements that include the dissolution of iron and silicon. These results clearly show that dissolution of iron from the clay as a result of chemical reduction in CB buffer is very small, and far below the 20 percent value suggested by Rozenson and Heller-Kallai (1976) in unbuffered solutions.

Table 2.1. The dissolution of Fe, Si, and Al during treatment with citrate-bicarbonate buffer (CB) and citrate-bicarbonate-dithionite (CBD).

Super- natant Solution	μmol/g clay							
	UPM		CZM		NZM		GAN	
	CB	CBD	CB	CBD	CB	CBD	CB	CBD
Fe								
Extract	3.16	13.35	--	153.07	0.62	38.33	2.72	75.02
1	0.30	1.95	--	45.73	4.80	5.10	1.19	3.27
2	0.29	0.00	--	48.17	2.11	14.68	1.27	1.35
3	0.00	0.00	--	39.63	1.05	10.74	0.82	1.34
4	2.01	0.00	--	20.84	1.50	8.01	0.82	1.29
Total	5.76	15.30	--	307.74	10.08	76.86	6.82	82.27
Si								
Extract	30.42	40.57	--	87.76	30.47	41.16	18.95	61.36
1	11.62	9.82	--	9.02	8.84	0.00	6.62	9.91
2	3.04	3.44	--	9.04	0.88	10.91	3.86	9.19
3	3.33	2.25	--	3.92	6.96	3.38	3.40	26.76
4	3.27	2.49	--	3.75	2.48	2.49	2.47	8.79
Total	51.68	58.59	--	113.49	49.63	57.94	35.30	116.01
Al								
Extract	24.15	14.77	--	25.14	18.81	22.98	13.12	13.20
1	299.51	243.18	--	21.43	474.94	66.59	35.13	11.26
2	187.29	188.67	--	266.16	303.71	516.69	34.11	10.84
3	210.62	161.32	--	271.10	88.52	168.57	16.40	17.96
4	189.68	155.37	--	111.52	99.44	165.11	6.97	7.37
Total	911.25	763.31	--	695.35	985.42	939.94	105.73	60.63

*Not Determined.

The dissolution data for aluminum (Tables 2.1 and 2.2) present quite a different picture than the data for iron and silicon. Dissolution was much more extensive, with as much as 26 percent of the aluminum being dissolved; the effects of CB and CBD were reversed; and the concentration in the initial extract was much lower than in the NaCl wash solutions. Even the supernatants from the fourth washings generally contained more aluminum than the extracts, raising the possibility

Table 2.2. The total quantities of Fe, Si, and Al dissolved from four smectites in 0.25 N citrate-bicarbonate buffer with (CBD) and without (CB) 200 mg of Na₂S₂O₄.

Amount of Element Dissolved														
Smectite	Treatment	% of Total Element				Weight % of Clay				Fe/Sit		Al/Sit		Unit-cell
		Fe	Si	Al	Fe	Si	Al	Total	Total as Oxides	Solution	Unit-cell	Solution	Unit-cell	
UPM	CB	1.34	0.49	20.91	0.03	0.14	2.46	2.63	5.15	0.11	0.04	17.63	0.41	
	CBD	3.56	0.56	17.51	0.08	0.16	2.06	3.20	4.53	0.26		13.03		
CZM	CB*	----	----	----	----	----	----	----	----	----	0.17	----	0.52	
	CBD	20.27	1.25	14.75	1.72	0.32	1.88	3.92	7.06	2.71		6.13		
NZM	CB	0.55	0.53	26.46	0.06	0.14	2.66	2.86	5.57	0.20	0.19	19.86	0.40	
	CBD	4.21	0.62	25.23	0.43	0.16	2.54	3.13	5.94	1.33		16.22		
GAN	CB	0.15	0.42	8.39	0.04	0.10	0.28	0.42	0.91	0.19	0.54	2.99	0.15	
	CBD	1.83	1.39	4.81	0.46	0.33	0.16	0.95	2.04	0.71		0.52		

*Not determined

†Mole Ratio

that more aluminum would have been solubilized if more washing cycles had been used. The very large mole ratios of Al/Si in solution, as compared to the unit-cell Al/Si ratios, indicate a strong selectivity for Al dissolution in the citrate-bicarbonate medium. The addition of dithionite decreases slightly the aluminum concentration in solution. These observations contrast sharply with the dissolution of iron and silicon, which was enhanced by the addition of dithionite.

These results seem to contradict the observed changes in surface charge. Since the surface charge is expressed as an intensive property of the system, it should be unaffected by homogeneous dissolution. But heterogeneous dissolution, which creates defects in the mineral structure, should alter the surface charge. The data clearly indicate that dissolution is heterogeneous, especially with respect to aluminum. If the large amounts of aluminum recovered in solution from the CB treated clays had been extracted from the clay structure as Al^{3+} , the surface charge would have increased several fold. But the surface charge of each unreduced clay in CB buffer agrees very well with previously published values and with the unit-cell formulas, showing no significant increase, and thus fails to support a heterogeneous dissolution model.

This apparent contradiction might be explained by proton adsorption. The charge deficit created by selective removal of Al^{3+} from structural sites may be balanced by the adsorption of three protons for each Al^{3+} dissolved, without changing the Na^+ counter-ion content. This would be undetected in this study because the method for surface charge determination assumes Na^+ is the only counter-ion. Initially the amount of Al^{3+} released in the buffer is rather low, but the presence of adsorbed protons could stimulate further dissolution of the structural Al^{3+} (Kamil and Shainberg, 1968; Shainberg, 1973). When the clay is washed with dilute NaCl solution, the pH drops from ~8 to ~6.8, thus further encouraging proton adsorption and continuation of the cycle. This also would explain the continued release of Al^{3+} through all washing cycles. The reversibility of the surface charge upon reoxidation is more difficult to rationalize, but would fit into this scheme if the decreased negative charge due to the oxidation of Fe^{2+} were balanced only by the desorption of Na^+ . Arguments against this model are that the Na^+ concentration in solution is $\sim 10^4$ greater than the H^+ concentration, so by mass action Na^+ would compete very strongly for "new" surface sites. To see no appreciable increase in exchanged Na^+ in unreduced, CB-treated samples would, therefore, appear to be unusual. Further, this model requires proton adsorption to be limited strictly to the neutralization of charge created by Al^{3+} dissolution, and Na^+ adsorption/desorption to be restricted to balancing the charge variations due to oxidation and reduction of iron. These requirements are rigid and perhaps unrealistic, but could be accommodated if the hydrogen ions replace the Al^{3+} in the crystal lattice of the clay (Paver and Marshall, 1934; Low, 1955; Shainberg et al., 1974). In any case, the observed surface charge appears to be independent of aluminum dissolution, but responds reversibly to changes in the iron oxidation state.

An alternative explanation might be that a separate aluminum phase exists in these clays and is dissolved preferentially to structural aluminum, thus accounting for the disproportionate amount of Al recovered in solution. Perhaps Fe and Si also are present in separate phases. However, acid dissolution studies using the method of Osthaus (1956) failed to detect any heterogeneity in the dissolution rates of either Al, Fe or Mg in the UPM sample so the possibility of a separate phase seems quite remote.

Two other explanations were considered, but seem untenable. The first was the readsorption of aluminum, iron or silicon. This is illogical since these ions are recovered in solution and cannot be in two places at one time. The other was that a sufficient number of oxide and/or hydroxide ions dissolve simultaneously with Al^{3+} to balance the charge deficit. If this had occurred, commensurate amounts of iron and silicon would have been observed in the CB solutions due to the destruction of the crystal lattice. The concentration of aluminum in the CB solutions was an order of magnitude greater than for the iron and silicon. This explanation also fails to account for reversibility.

2.4. Summary

The reduction of structural ferric iron in the octahedral sheet of dioctahedral smectites produced a net increase in the negative surface charge of the clay. The observed values deviated from the relationships predicted by charge deficit calculations, and a finite maximum charge was reached for each clay studied. This effect is reversible. Small amounts of iron and silicon were dissolved during the reduction treatment, but this affects less than one percent of the total clay mass, except in the CZM clay where approximately two percent of the clay was dissolved as iron and silicon. Dissolution with respect to these ions appears to be sufficiently homogeneous to have little or no effect on the net surface charge.

In contrast, extensive amounts (as much as 26 percent) of aluminum were selectively dissolved in the citrate-bicarbonate solution. This heterogeneous pattern, however, was completely undetected by the surface charge measurements. The hypothesis accounting for this phenomenon is that adsorbed hydrogen ions balance the charge deficit created by aluminum dissolution, which in turn stimulates further aluminum release from the clay structure. Aluminum dissolution appears to be largely independent of the redox reactions, and the effects of iron oxidation state on the surface charge cannot be explained by it.

3. The Effects of Iron Oxidation State on Clay Swelling

3.1. Introduction

Some evidence indicates that it might be possible to control clay swelling by altering the oxidation state of the iron in the octahedral sheet of the clay crystal. Foster (1953) reported a direct, but qualitative relationship between swelling and the oxidation state of octahedral iron. Using freshly mined Wyoming bentonite (Belle Fourche), she observed that the swelling volume of the blue-grey (reduced) fraction, measured in a graduated cylinder, was about two-thirds that of the olive-green (oxidized) fraction. Other, less-direct evidence is found by comparing the works of Ravina and Low (1972, 1977) with the work of Kohyama *et al.* (1973). The latter group reported a larger b-dimension for the reduced form of saponite than for the oxidized form. Ravina and Low observed an empirical, inverse relationship between b-dimension and swelling. Putting these observations together, one would conclude that iron reduction should decrease swelling. This conclusion is consistent with Foster's observation.

Using the methods, apparatus and understanding achieved from the results reported in sections 1 and 2 above, the effects of iron oxidation state on swelling were demonstrated under carefully controlled conditions. Following are the results of that study.

3.2. Methods

The clays were suspended in 0.25 N citrate-bicarbonate (CB) solution in a special reaction vessel (Fig. 1.1) having a septum cap, then prepared in various states of oxidation using the methods and apparatus described in section 1 above. The solute concentration in the final suspension was $\sim 5 \times 10^{-4}$ mol/L Na^+ . To measure the swelling pressure of the clays, a swelling pressure manifold similar to the one described by Low (1980) was used. Two modifications were made to his design, however, and are illustrated in Fig. 3.1. The first modification was in the swelling pressure cell itself. Since the time when Low obtained plastic cells commercially, the quality control in their manufacture was lost and it was no longer possible to obtain commercially manufactured cells that would seal at the base. Hence, it was necessary to manufacture new cells in a University of Illinois instrument shop, based on a slightly different design but having essentially the same volume and principle of operation. The cells were constructed of stainless steel, and the inside surface of each barrel was coated with teflon.

In order to inject air sensitive samples into the swelling pressure cells with minimal exposure to atmospheric oxygen, a second modification was introduced. In the modified design (Fig. 3.1) a ball valve and adapter block were placed between the pressure cell and the needle valve, whereas in the original design (Low, 1980) the cell was attached directly to the needle valve. The opening in the ball valve and the overall length of the entire cell and valve assemblies were

PRESSURE CELL FOR SWELLING PRESSURE DETERMINATIONS

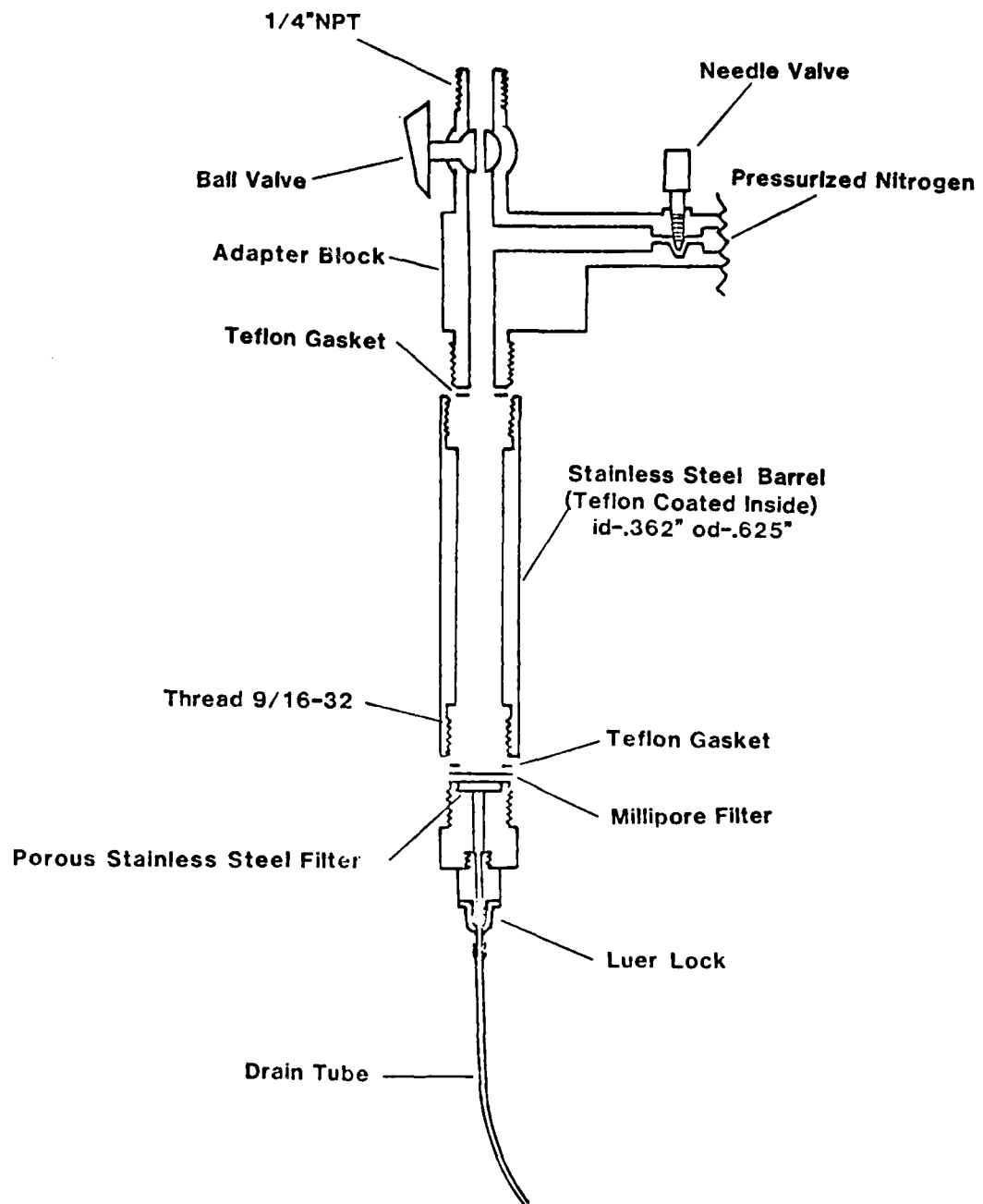


Figure 3.1 Schematic drawing of the swelling pressure cell and adapter block, modified from the design used by Low (1980).

such that, when assembled, the inside base of the cell could be reached from the top with a six-inch needle through the ball valve. The utility of this design for injecting air-sensitive samples will become more apparent in the procedure outlined below.

Prior to each swelling run, the cell base and barrel were disassembled, washed in deionized water (18 megohm/cm resistivity) and allowed to drain for several hours. Then the barrel was screwed onto the adapter block after inserting a teflon gasket to ensure air-tightness. A 13 mm millipore filter (0.025 μ m pore diameter) was placed on the porous stainless steel filter, and the entire cell base was saturated in its upright position by passing degassed water through the drain tube with a syringe until the air was expelled and the filter was saturated. The syringe was carefully removed while extruding water so no air bubbles would form in the drain tube. After removing the syringe, a teflon gasket was placed on top of the filter and the cell base was screwed into the barrel. Care was taken to have the ball valve open while the base was being attached to the barrel in order to maintain atmospheric pressure above the water-saturated filter and base.

Once the manifold was pressurized to the desired pressure (i.e., 0.101, 0.303, 0.505, or 0.707 MPa) and the cell was assembled and in place, the cell was flushed with oxygen-free nitrogen gas from the manifold by opening the needle valve. Since the ball valve was already open, the pressure in the cell remained atmospheric and a constant flow of nitrogen was established through the cell and out the ball valve. With the apparatus in this configuration, a 2.5 ml aliquot of the sample suspension was transferred from the reaction vessel to the pressure cell using a gas-tight syringe and six-inch long needle. Immediately following the transfer, the ball valve was closed and the cell thus became pressurized with the pressure previously established in the manifold.

Equilibrium was determined by monitoring the effluent flow rate from the drain tube. This was facilitated by a thin glass capillary tube attached to the end of the drain tube. There was no definite criterion to establish a sharp end point, but the first appearance of the slower water movement was taken as a practical guide. At lower pressures a stationary flow was the criterion, but at higher pressures diffusion of nitrogen into the drain through the filter and clay cake caused a continuous movement of the water column. Occasionally, tiny air bubbles would appear in the drain tube as the system approached equilibrium.

Three aliquots from each sample were transferred to separate ports on the manifold, using the same procedure at each port, and a maximum of three samples (nine ports) were used in each run. The limiting factor was the number of ports (ten) on the manifold. After equilibrium was reached, the water contents of the gels from two of the three ports used for each sample were determined as follows. The needle valve was closed and the cell base removed, then the gel was quickly transferred to a 75 mm x 15 mm weighing bottle, covered, weighed, oven-

dried at 110 C and weighed again. From the gel weight before (m_g) and after (m_d) oven drying, the water content (m_w/m_c) was calculated using the equation

$$\frac{m_w}{m_c} = \frac{m_g}{m_d} - 1 \quad [3.1]$$

The dried gels were then digested and analyzed for total iron using the method described by Stucki (1981). The gel from the third cell was removed in like manner but transferred to a previously prepared digest solution in a 100 ml polypropylene centrifuge tube for the determination of the ferrous to total iron ratio (Stucki, 1981). Relative values for Fe^{2+} and total Fe were converted to a clay-weight basis by multiplying by the total iron content of the dried gels.

3.3. Results and Discussion

The water content of the clays UPM, CZM, NZM, and GAN was determined at four different applied swelling pressures, Π , with the clays in various states of oxidation. The results reported in Table 3.1 and Fig. 3.2 reveal a marked decrease in the equilibrium water content as the ferrous iron composition increases. The mathematical form of this effect is clearly linear in the UPM and CZM clays, but appears somewhat more complicated in the NZM and GAN samples. In these last two the water content decreases rapidly during the initial stages of reduction, then levels off until further reduction invokes little or no additional change in water content. In Fig. 3.2, the data for these clays are fitted to a curvilinear line, but likely could be described as well or better by two straight lines intersecting in the neighborhood of 0.40 mmol Fe^{2+} /g clay. The region of the curve above this point ($Fe^{2+} > 0.40$ mmol/g) clearly obeys a linear equation of near zero slope. For the region below it the number of data are insufficient for a complete statistical treatment, but linear regression analysis of the available points yields very high correlation coefficients (Table 3.2). This is particularly significant because the full range of ferrous compositions studied with UPM and CZM samples, which yielded a linear response, was entirely below 0.40 mmol Fe^{2+} /g, suggesting that all of the clays behave uniformly and if iron reduction in the UPM and CZM samples were to exceed 0.40 mmol Fe^{2+} /g, perhaps a similar levelling off would be observed.

The initial slopes of the lines in Fig. 3.2 (whether linear or curvilinear) provide a means to evaluate the sensitivity of the water content to changes in iron oxidation state. By comparing the linear regression coefficients (slopes) of the lines in the range 0-0.4 mmol Fe^{2+} /g (Table 3.2), differences in the clays are immediately apparent. The greater the absolute value of the slope, the more responsive the clay-water ratio is to iron oxidation state. On this basis, the relative sensitivities of the four clays used in this study increases in the order CZM < UPM < GAN < NZM. Notice that this order fails to correspond to the order of variation in other characteristics such as total iron composition (UPM < CZM < NZM < GAN), surface charge (CZM <

Table 3.1. The ferrous iron content and corresponding mass ratios of water to clay, m_w/m_c , in equilibrium with various applied swelling pressures, Π .

		Π , MPa							
Total Fe		0.101		0.303		0.505		0.707	
Smectite	mmol/g	Fe ²⁺ mmol/g	m_w/m_c (g/g)	Fe ²⁺ mmol/g	m_w/m_c (g/g)	Fe ²⁺ mmol/g	m_w/m_c (g/g)	Fe ²⁺ mmol/g	m_w/m_c (g/g)
UPM	0.539	0.016 0.150 0.224	4.591* 4.337+ 4.233	0.042 0.204 0.207 0.250 0.370	2.273 2.086+ 2.083+ 2.033 1.883	0.014 0.147 0.165	1.636* 1.532+ 1.492	0.053 0.304 0.367 0.391	1.379* 1.125 1.049 1.025
CZM	1.257	0.004 0.262 0.329	2.300* 2.009+ 1.951	0.084 0.123 0.157	1.290* 1.260+ 1.240	0.004 0.133 0.224	1.091* 1.020+ 0.975	n. d. n. d.	n. d.
NZM	1.502	0.036 0.097 0.108 0.755 0.852	3.073+ 2.660 2.600 1.810 1.770	0.005 0.136 0.759	1.743* 1.202+ 0.893	0.010 0.030 0.102 0.821 0.874	1.291* 1.205+ 0.995 0.680 0.690	0.007 0.385 0.721	1.162* 0.581+ 0.563
GAN	4.201	0.020 0.737 1.540 1.697 1.983	3.400 2.275 2.191 2.175 2.145	0.008 1.128 1.228 3.109 3.188	1.712* 1.128+ 1.126+ 1.026 1.025	0.014 0.018† 0.035 0.308 1.367 2.161† 2.328 2.566† 2.950† 3.274†	1.327* 1.256* 1.245 1.021 0.875 0.869 0.836 0.854 0.846 0.850	0.007 0.019 0.216 0.948 2.376	1.144* 1.125+ 0.975+ 0.770 0.751

†Reduced for 7 days.

*Unreduced

+Reduced then reoxidized

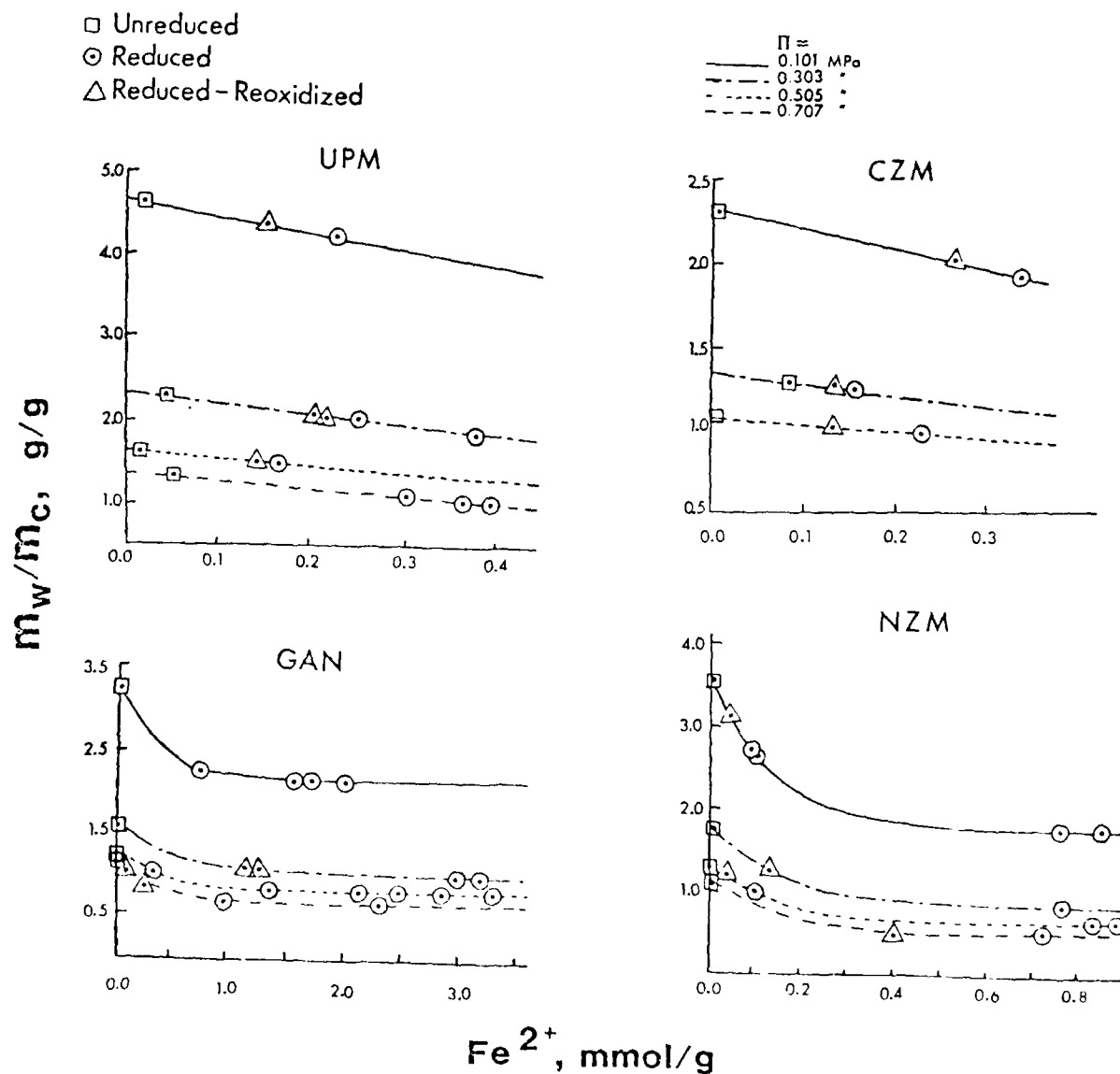


Figure 3.2 The equilibrium water content, m_w/m_c , at various applied swelling pressures, Π , for smectites in various states of iron oxidation.

Table 3.2. Correlation coefficients (r^2) and slopes (c) of m_w/m_c versus ferrous iron composition in the range 0-0.40 mmol Fe^{2+}/g clay.

Smectite	Swelling Pressure, MPa							
	0.101		0.303		0.505		0.707	
	r^2	-c	r^2	-c	r^2	-c	r^2	-c
UPM	0.9948	1.742	0.9994	1.186	0.9736	0.889	0.9992	1.045
CZM	0.9997	1.111	0.9943	0.687	0.9991	0.529	#	#
NZM	0.9993	6.637	1.0000*	4.130	0.9939	3.137	1.0000*	1.537
GAN	#	#	#	#	0.8117	0.201	0.9973	0.788

#less than two points in the range

*only two points in the range

UPM < NZM < GAN), or the substitution of Al for Si in the tetrahedral sheet (CZM > GAN > NZM > UPM).

The uniformity of the individual curves in Fig. 3.2 suggests that the effect of iron oxidation state on water content is reversible. The results reported in this Figure (and in Table 3.1) represent clays in CB buffer solution that were reduced, reduced then reoxidized, or unreduced. One set of GAN samples was treated for seven days to gauge the effect of time in the reaction medium (including CB buffer without dithionite) on the relationship between ferrous iron composition and water content. Since all points for a given clay at the same pressure fit nicely on the same line (or lines if two linear regions exist) regardless of the sample history, the water content must depend only on the state of oxidation, and not on the path by which that state was reached. Treatment of the clay with citrate-bicarbonate and with dithionite dissolves some Fe, Si, and Al from the clay structure (see section 2 above), and raises the possibility that changes in water content might be attributable to mineralogical alterations other than the reduction of structural ferric iron. However, since the observed water content reversibly follows the changes in iron oxidation state, any irreversible dissolution of metal ions from the structure either must occur homogeneously or, if heterogeneous, must follow a mechanism that has no detectable influence on water properties.

Swelling pressure curves were constructed from Fig. 3.2 by graphically determining the corresponding values of m_w/m_c from the curves

for the different applied pressures. The values of Π were then plotted against m_w/m_c for 0, 0.25, 0.36, and 0.90 mmol Fe^{2+}/g clay (Fig. 3.3). The observed shifts in position of the swelling pressure curves are distinct and substantial, especially in the range of 0-0.4 mmol Fe^{2+}/g , and demonstrate that the reduction of structural iron markedly decreases the swelling pressure of the clay. The magnitude of this effect was determined by comparing the pressures required to achieve the same water content in the various reduced states of each clay (Table 3.3). A change in iron oxidation state from 0 to 0.36 mmol Fe^{2+}/g decreased the swelling pressure 22%, 31%, 39%, and 56% for the respective clays UPM, CZM, GAN, and NZM containing 1.5 g H_2O/g clay. For such a relatively small change in the iron oxidation state, which affects less than two percent of the total clay weight, these changes in swelling pressure are profound.

Table 3.3. The surface charge, ω , and swelling pressure, Π , of UPM, CZM, NZM, and GAN smectites in various states of reduction. The values for Π were obtained graphically from Fig. 3.3 at $m_w/m_c = 1.5$ g/g. The values for ω were obtained graphically from Fig. 2.1.

Smectite	Specific Surface Area* $cm^2/g \times 10^{-6}$	Fe^{2+} mmol/g	Π MPa	ω	
				mmol(Na^+)/g	esu/ $g \times 10^{-11}$
UPM	8.00	0	0.561	0.86	2.487
		0.25	0.490	1.11	3.210
		0.36	0.435	1.17	3.384
CZM	4.38	0	0.255	0.49	1.417
		0.25	0.200	0.63	1.822
		0.36	0.177	0.66	1.909
NZM	4.50	0	0.405	0.80	2.314
		0.25	0.197	0.87	2.516
		0.36	0.178	0.91	2.632
		0.90	0.150	0.97	2.805
GAN	7.08	0	0.395	1.04	3.008
		0.25	0.270	1.24	3.586
		0.36	0.240	1.32	3.818
		0.90	0.198	1.53	4.425

*Low, 1980.

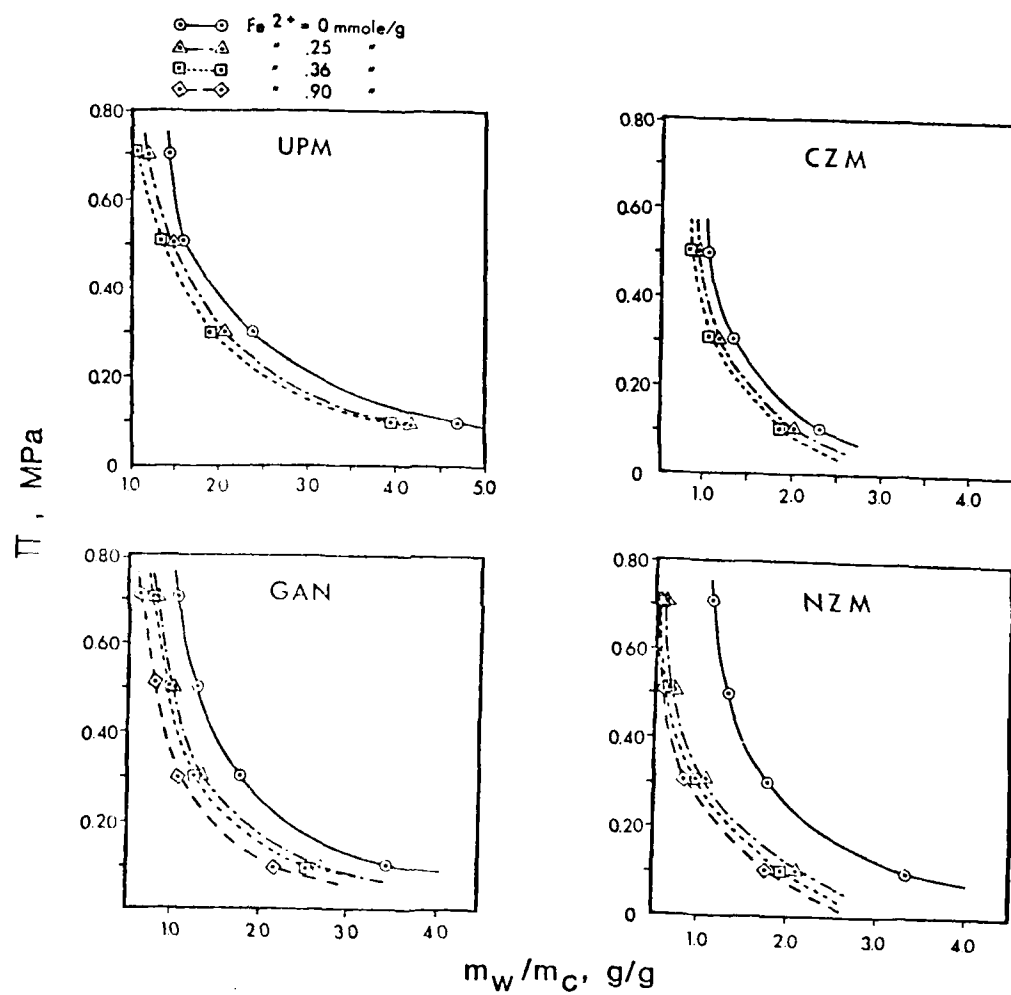


Figure 3.3 The effect of iron oxidation state on the swelling pressure curves of Na⁺-smectites in 5×10^{-4} N NaCl solution.

To explain these observations the following physical model is proposed. The reduction of ferric iron in the clay crystals causes some of the layers to collapse to form packets of partially or non-expanding layers, such as suggested by Norrish (1954), forcing most of the water from their interlayer spaces. These vermiculite-like packets swell only from their outermost surfaces. In effect, the system consists of some particles that exhibit limited or "type 1" swelling (MacEwan, 1960) mixed with others that undergo complete or "type 2" swelling. Upon reoxidation the complete swellability of most, if not all, of the previously swelling layers is restored and the packets are "dissolved."

This model is supported by arguments based on two different theories of clay swelling, namely, Low's empirical equation (Low and Margheim, 1979), and DLVO theory. For many years Low and co-workers have advocated that swelling is a surface phenomenon rather than a result of osmotic forces as required by the Langmuir (1938) equation in the DLVO theory (van Olphen, 1963; Verwey and Overbeek, 1948). Their early work revealed that many physical properties of bulk water are changed when it is adsorbed between layers of Na^+ -montmorillonite (e.g., Oster and Low, 1964; Kolaian and Low, 1960; Davidtz and Low, 1970; Ravina and Low, 1977; Low, 1976; Ruiz and Low, 1976; Odom and Low, 1978). Low and Margheim (1979) developed an empirical equation relating the swelling pressure to the water content:

$$\ln(\Pi+1) = \ln(\beta) + \alpha m_c/m_w \quad [3.2]$$

where α and β are constants that depend on the properties of the clay. The value of α depends directly on the specific surface area of the clay. To determine whether the data from the present study fit this empirical equation, Fig. 3.4 was constructed by plotting the experimental values of m_c/m_w from Fig. 3.3 versus the corresponding values for $\ln(\Pi+1)$. With only three or four points a rigorous statistical test was not possible, but the existing points do seem to fit either one or two straight lines. Low (1980) studied these same clays in their natural (oxidized) oxidation state and found that they all obey equation [3.2]. He also observed two different linear regions with several clays, including UPM and NZM. Thus the two linear regions seen in some of the lines in Fig. 3.4 are not without precedent and appear to be consistent with previous observations. However, no distinct pattern emerges to predict in which lines a break should occur. The CZM samples showed no sign of a break with the three available points, which is also consistent with earlier results (Low, 1980). Another interesting observation from Fig. 3.4 is that the principal difference between the respective lines for each clay appears to be the slope, which decreases with increasing ferrous iron content. Since the slope (α) varies directly with surface area in a host of unreduced smectites (Low, 1980), it seems reasonable that the surface area is likewise decreasing in these samples as the ferrous content rises. Further, it has been demonstrated theoretically (Low, 1980) and by low-angle x-ray diffraction measurements (Viani et al., 1982, ACS Symposium on the Physico-Chemical Properties of Clays, Las Vegas, Nevada, Book of

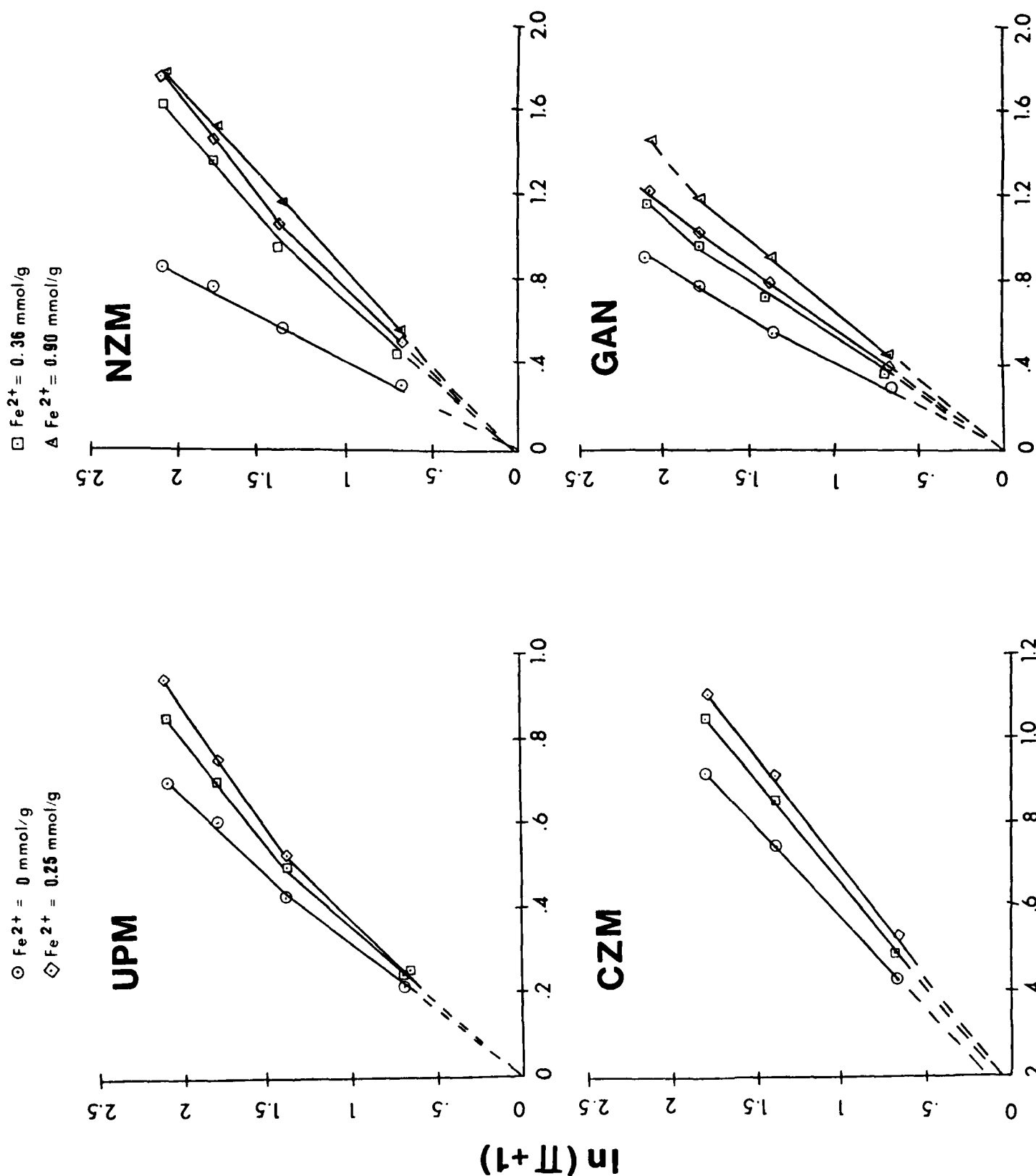


Figure 3.4 The relation between $\ln(\Pi+1)$ and m_c/m_w for the UPM, CZM, NZM, and GAN smectites in several different states of iron oxidation.

Abstract, COLL 162) that at any given applied swelling pressure the interlayer distance (c-axis spacing) is constant regardless of the clay and its water content. The equation is

$$n+1 = B \exp [k/\lambda] \quad [3.3]$$

where B and k are constants. Neither this relationship nor the suggested decrease in surface area has been confirmed experimentally for reduced samples, but since the experimental data appear to obey equation [3.2], it is reasonable to assume that these clays behave in a manner similar to those studied by Low and co-workers. It follows, then, that the iron oxidation state in some manner alters or controls the surface area of the clay. And if the c-axis spacing is constant at a given applied pressure (equation [3.3]), regardless of oxidation state, then changes in water content must be due to changes in the number of, rather than the distance between, expanding layers.

The mechanism by which iron oxidation state controls surface area likely is related to the effect of surface charge on the number of collapsed layers. As described above in section 2, we also observed a reversible increase in surface charge (ω) which closely parallels the reversible decrease in swelling pressure with reduction. Fig. 3.5 illustrates this inverse relationship between swelling pressure and surface charge. It is reasonable to believe that increasing the charge causes some layers to collapse since the low expandability of vermiculites is generally attributed to their higher charge relative to smectites (MacEwan, 1955), and is consistent with Weiss' (1958) observation that in micaceous silicates the interlayer spacing in distilled water decreases with increasing surface charge density. The range of surface charge values for the clays in this study extend into the lower end of the observed (Foster, 1963) range for naturally-occurring vermiculites, but the apparent collapse of layers clearly must occur below this range as well. Perhaps for layers to collapse in any given clay, the ratio of reduced to oxidized (natural) charge is a more dominant factor than the absolute value, so the critical surface charge above which a clay will "vermiculitize" is a function of the relative rather than the absolute value of the charge.

The results reported in Fig. 3.5 are inconsistent with DLVO theory if the surface area is unaffected by iron reduction. This arises from the fact that the Langmuir (1938) equation requires a direct dependence of repulsive pressure on the surface charge density. We observe an inverse dependence (Fig. 3.5), assuming the planar surface area of individual layers is constant. Hence, we are forced to conclude that the Langmuir (1938) equation does not describe the effects of iron oxidation state on clay swelling. Possible reasons for this include: a) swelling is not osmotic; or/and b) the Langmuir equation has no provision to account for variations in the number of collapsed versus expanding layers.

It may be possible that iron reduction alters two different properties of the system that affect swelling in opposite directions. The

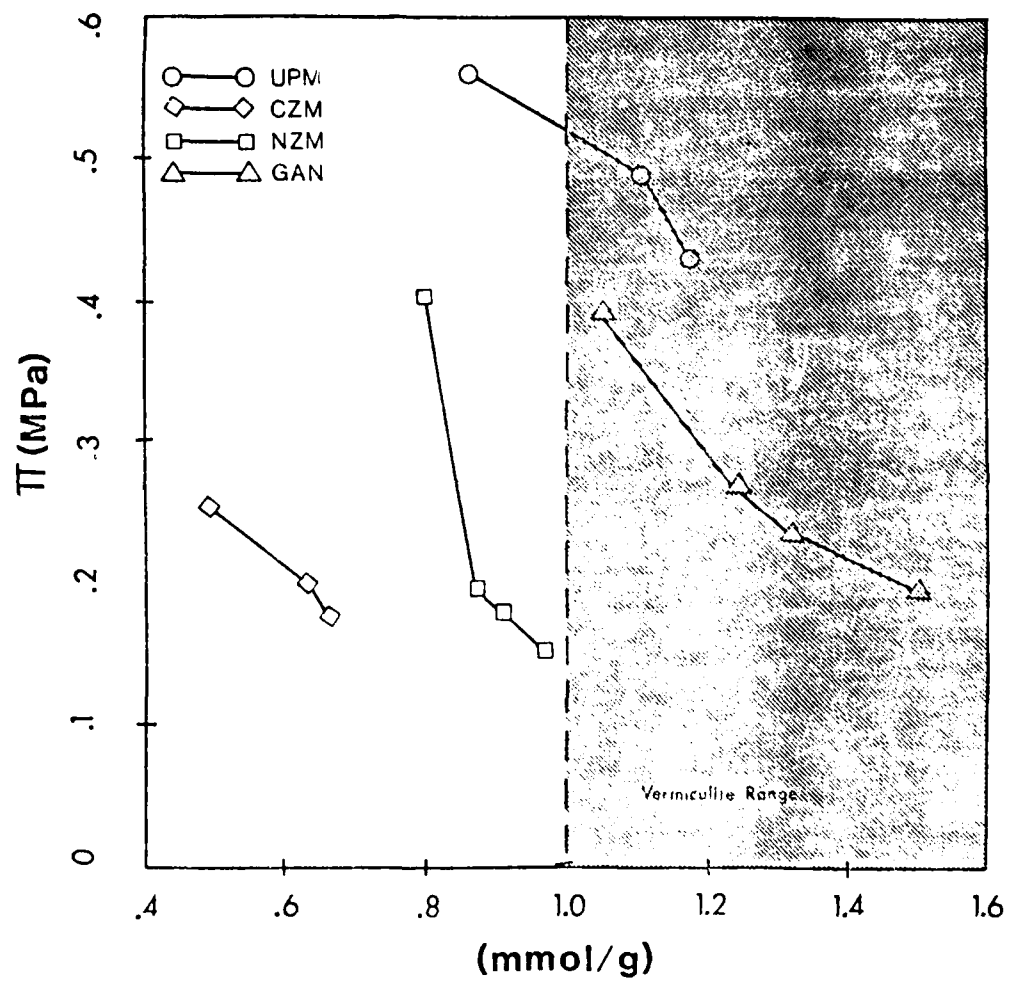


Figure 3.5 The observed relation between Π and the surface charge, ω .

increased negative charge on the clay layer will produce a greater surface charge density in the interfacial region of that individual layer. According to DLVO theory, this should increase the swelling pressure and consequently the water volume associated with that particular interlayer region. On the other hand, the increased charge also can cause the layers to collapse as observed in the case of vermiculite, which would decrease the water volume in the interlayer space. Perhaps more layers collapse during iron reduction than would be necessary to counter the increased water content predicted by DLVO theory for the surfaces participating in osmotic swelling. The result would be a net decrease in the total water content.

If swelling is indeed osmotic, but some layers are allowed to collapse as proposed above in the description of the physical model, then it should be possible to estimate the fraction of collapsed layers in the system from DLVO theory equations using the equilibrium water content and surface charge values reported in Tables 3.1 and 3.3. For this purpose assume the total water content of the system can be divided into three components (Fink *et al.*, 1968): the intracrystalline water, $(m_w)_{\text{intra}}$, that which is between the collapsed layers, the intercrystalline water, $(m_w)_{\text{inter}}$ that which is between the freely expanding layers; and the external water; $(m_w)_{\text{ext}}$, that which is in pore spaces external to the interlaminar regions of the clay. Fink *et al.* (1968) estimated that the external water in Na^+ -montmorillonite accounted for about 13% of the total water content in the free-swelling state. We can therefore express the total water content of the system in terms of these various components as

$$\frac{(m_w)_T - (m_w)_{\text{ext}}}{m_c} = \left(\frac{m_w}{m_c}\right)_{\text{intra}} + \left(\frac{m_w}{m_c}\right)_{\text{inter}} \quad [3.4]$$

If a_i is the total planar surface area of a single layer, and λ the distance between layers, the amount of water between the layers can then be written

$$m_w = \sum_i \rho \lambda a_i / 2 \quad [3.5]$$

where ρ is the density of the water, and the factor 2 accounts for the fact that the water lies between two parallel plates. If λ is constant, or if the average quantity is used, equation [3.5] can be rewritten

$$m_w = \frac{\rho \lambda}{2} \sum_i a_i. \quad [3.6]$$

Notice that the specific surface area is defined by $S = \sum_i a_i / m_c$, where m_c is the mass of clay. After rearranging this relation and substituting for $\sum_i a_i$, equation [3.6] becomes

$$\frac{m_w}{m_c} = \rho \lambda S / 2 \quad [3.7]$$

The total planar surface area can be proportioned between the surfaces associated with freely expanding layers and those associated with limited expanding layers according to the fractions $1-f$ and f , respectively. Now if we assume that the c -axis spacings of these two different types of expanding layers are constant for a given applied swelling pressure, and are represented by λ and λ_0 , respectively, then the right hand side of equation [3.4] can be written

$$\left(\frac{m_w}{m_c}\right)_{\text{intra}} + \left(\frac{m_w}{m_c}\right)_{\text{inter}} = \rho f \lambda_0 S/2 + \rho (1-f) \lambda S/2 \quad [3.8]$$

Equation [3.4] can therefore be written, after substitution of equation [3.8] on the right hand side,

$$\frac{(m_w)_T - (m_w)_{\text{ext}}}{m_c} = \rho \lambda_0 f S/2 + \rho \lambda (1-f) S/2 \quad [3.9]$$

Solving this equation for f yields

$$f = \left[\frac{2(m_w)_T - 2(m_w)_{\text{ext}}}{\rho S m_c} - \lambda \right] / (\lambda_0 - \lambda) \quad [3.10]$$

Equation 3.10 was evaluated for all of the clays in this study with 0 and 0.36 mmol Fe^{2+}/g , using the observed surface charge values (Table 3.3) and total water contents, and assuming the ideal surface area of $8 \times 10^6 \text{ cm}^2/\text{g}$. As a first approximation, it was assumed that the external water content was that of Na^+ -montmorillonite (13%) reported by Fink et al. (1968), and the separation of collapsed layers was 9 \AA (~ 4 water layers). Values for λ were then calculated from DLVO theory using the tables of van Olphen (1963) and the appropriate values of κ and σ from the present experiment. Corrections for the van der Waal's attractive forces were made after the procedure of Low (1980). The corresponding values of f for oxidized and reduced samples at four different pressures are compiled in Table 3.4. These results indicate that in reduced samples approximately more than half of the surface area is associated with a collapsed environment, consistently more than in the oxidized samples. If the interlayer spacing of the collapsed layers were to be less than 9 \AA , then of course the fraction of collapsed layers would have to increase accordingly in order to account for the decreased water content in the interlaminar regions, and the packets would on the average consist of more than two layers. These effects should be detectable by low-angle x-ray diffraction.

3.4. Summary

The effect of iron oxidation state on clay swelling is pronounced. A change of only 0.36 mmol Fe^{2+}/g clay alters the swelling pressure by as much as 56%, depending on the clay. All clays studied behave uniformly and most of the effect occurs below 0.40 mmol Fe^{2+}/g . The total iron composition and the site of isomorphous substitution appear to

Table 3.4. The estimated fraction of collapsed layers calculated from eq. [3.10] using DLVO theory to estimate λ . Units of Π are MPa.

Smectite	Fe ²⁺ mmol/g	f			
		$\Pi = 0.101$	$\Pi = 0.303$	$\Pi = 0.505$	$\Pi = 0.707$
UPM	0	-0.13	-0.02	0	-0.12
	0.36	0.06	0.25	0.30	0.33
CZM	0	0.45	0.39	0.30	-----
	0.36	0.58	0.60	0.57	-----
NZM	0	0.21	0.26	0.25	0.13
	0.36	0.59	0.71	0.79	0.83
GAN	0	0.20	0.30	0.31	0.28
	0.36	0.45	0.57	0.57	0.60

have little or no effect on the swelling properties. The swelling pressure versus water content relations appear to obey Low's empirical equation of swelling, which suggests that the reduction of iron in the clay crystals decreases the specific surface area of the clay. The proposed physical model describing this process is that the reduction of iron causes some of the layers to collapse, thereby decreasing the number of swelling surfaces available to the water. The observed increase in surface charge may be the major factor controlling the collapse of the layers. The observed relationship between swelling pressure and surface charge density is inverse, contrary to the direct relationship required by the Langmuir (1938) equation in DLVO theory.

4. The Relation Between c-axis Spacings and Water Contents of Clay Gels at Various Applied Swelling Pressures.

Some of the research in this project was performed under a subcontract with Philip F. Low and Charles B. Roth at Purdue University. A major portion of their work focussed on the measurement of the crystallographic c-axis spacings of clay gels as a function of applied swelling pressure, Π . The results are extremely interesting and form additional ground-work for possible further investigations with regard to the effects of iron oxidation state on clay swelling. For these reasons a summary of their results are reported here. The following summary was written by Dr. Low.

In order to fully describe swelling in smectite-water systems, a direct measure of interlayer distances, λ , as a function of applied swelling pressures, Π , is necessary. Previous measurements of macroscopic swelling in smectites has shown that the mass ratio of water to clay, m_w/m_c , is related to the applied swelling pressure, Π , by:

$$\ln(\Pi+1) = \alpha(1/m_c/m_w) + \ln\beta \quad [4.1]$$

where α and β are constants characteristic for each sample. It was proposed that the interlayer separation, λ , would also be related to Π in the same way that m_w/m_c is.

The interlayer spacing was measured as a function of Π for a series of smectites ranging in charge density from 27,000 to 56,000 esu/cm². Highly oriented samples were prepared by sedimentation onto a membrane filter and x-rayed using a diffractometer equipped with an environmental chamber with beryllium windows. A drain from the filter support led to the outside of the environmental chamber. This allowed determination of c-axis spacings at pressures up to 0.7 MPa. X-ray data were digitally collected for each sample after equilibration at each successively greater pressure. The data were transferred to a computer, analyzed, and c-axis spacing and interlayer spacing computed.

The results of the study to date are:

1. The interlayer spacing, λ , is related to Π as shown in equation [4.2] that is:

$$\ln(\Pi+1) = K(1/\lambda) + C, \quad [4.2]$$

where K and C are constants characteristic for a particular clay.

2. For any given pressure Π , the measured λ 's are similar for all the samples and are therefore independent of surface charge density.
3. The observed relationship between Π and λ is much different in form and magnitude from that predicted by DLVO theory,

and therefore cannot be explained by it. It is clear that there are repulsive forces operating between smectite sheets that arise independently from any double layer forces that may be present. These repulsive forces are attributed to the adsorption of water by the particle surfaces.

The effect of oxidation states of structural Fe on the relationship of Π versus λ can now be studied. The measurement of λ 's for reduced clays will show whether the differences observed in the macroscopic swelling between reduced and oxidized systems is the result of changes in the relationship of Π versus λ , or due to changes in the proportion of collapsed and expanding layers.

LIST OF PUBLICATIONS

1. The Quantitative Assay of Minerals for Fe^{2+} and Fe^{3+} Using 1, 10-Phenanthroline. I. Sources of Variability. Soil Sci. Soc. Amer. J. 45:633-637. Joseph W. Stucki and Warren L. Anderson. (See Appendix A)
2. The Quantitative Assay of Minerals for Fe^{2+} and Fe^{3+} Using 1, 10-Phenanthroline. II. A Photochemical Method. Soil Sci. Soc. Amer. J. 45:638-641. Joseph W. Stucki. (See Appendix A)
3. The Preparation and Handling of Dithionite-Reduced Smectite Suspensions. Submitted to Clays Clay Miner. Joseph W. Stucki, D. C. Golden, and Charles B. Roth.
4. The Effects of Citrate-Bicarbonate-Dithionite Reduction and the Reoxidation of Structural Iron on the Surface Charge and Dissolution of Dioctahedral Smectites. Submitted to Clays Clay Miner. Joseph W. Stucki, D. C. Golden, and Charles B. Roth.
5. The Effect of Iron Oxidation State on Clay Swelling. Submitted to Clays Clay Miner. Joseph W. Stucki, Philip F. Low, Charles B. Roth, and D. C. Golden.
6. X-ray Determination of the Relation between Swelling Pressure and Interlayer Distance for Smectites. Manuscript in preparation. Brian E. Viani, Charles B. Roth, and Philip F. Low.

PARTICIPATING SCIENTIFIC PERSONNEL

1. Joseph W. Stucki, Associate Professor of Soil Science,
University of Illinois, Urbana, IL 61801
2. Philip F. Low, Professor of Soil Science, Purdue University
West Lafayette, IN 47901
3. Charles B. Roth, Associate Professor of Soil Science, Purdue
University, West Lafayette, IN 47901
4. D. C. Golden, Research Associate, University of Illinois,
Urbana, IL 61801
5. Brian E. Viani, Research Associate, Purdue University, West
Lafayette, IN 47901
6. Rose M. Pilgrim, Assistant Soil Chemist, University of
Illinois, Urbana, IL 61801

V. BIBLIOGRAPHY

- Davidtz, J. C., and Low, P. F. (1970) Relation between crystal-lattice configuration and swelling of montmorillonite: *Clays Clay Miner.* 18, 325-332.
- Fink, D. H., Rich, C. I., and Thomas, G. W. (1968) Determination of internal surface area, external water, and amount of montmorillonite in clay-water systems: *Soil Sci.* 105, 71-77.
- Foster, M. D. (1953) Geochemical studies of clay minerals: II. Relation between ionic substitution and swelling in montmorillonites: *Am. Mineral.* 38, 994-1006.
- Foster, M. D. (1963) Interpretation of the composition of vermiculites and hydrobiotites: *Clays Clay Miner.* 10, 70-89.
- Gast, R. G. (1977) Surface and colloid chemistry: In *Minerals in Soil Environments*, J. B. Dixon and S. B. Weed, eds., *Soil Sci. Soc. of Am.*, Madison, Wisconsin, 27-73.
- Kamil, J. and Shainberg, I. (1968) Hydrolysis of sodium montmorillonite in sodium chloride solutions: *Soil Sci.* 106, 193-199.
- Kohyama, N., Shimoda, S., and Sudo, T. (1973) Iron-rich saponite (ferrous and ferric forms): *Clays Clay Miner.* 21, 229-237.
- Kolaian, J. H., and Low, P. F. (1960) Thermodynamic properties of water in suspensions of montmorillonite: *Clays Clay Miner.* 9, 71-84.
- Langmuir, I. (1938) The role of attractive and repulsive forces in the formation of tactoids, thixotropic gels, protein crystals and coacervates: *J. Chem. Phys.* 6, 873-896.
- Low, P. F. (1955) The role of aluminum in the titration of bentonite: *Soil Sci. Soc. Amer. Proc.* 19, 135-139.
- Low, P. F. (1976) Viscosity of interlayer water in montmorillonite: *Soil Sci. Soc. Am. J.* 40, 500-505.
- Low, P. F. (1980) The swelling of clay--II: Montmorillonites: *Soil Sci. Soc. Am. J.* 44, 667-676.
- Low, P. F. (1981) The swelling of clay--III: Dissociation of exchangeable cations: *Soil Sci. Soc. Am. J.* 45, 1074-1078.
- Low, P. F. and Margheim, J. F. (1979) The swelling of clay--I: Basic concepts and empirical equations: *Soil Sci. Soc. Am. J.* 43, 473-481.
- MacEwan, Douglas M. C. (1955) Interlamellar sorption by clay minerals: *Clays Clay Miner.* 1, 78-85.

- MacEwan, Douglas M. C. (1960) Interlamellar reactions of clays and other substances: *Clays Clay Miner.* 9, 431-443.
- Norrish, K. (1954) The swelling of montmorillonite: *Disc. Faraday Soc.* 18, 120-134.
- Odom, J. W. and Low, P. F. (1978) Relation between swelling, surface area and b dimension of Na-montmorillonites: *Clays Clay Miner.* 26, 345-351.
- Oster, J. D., and Low, P. F. (1964) Heat capacities of clay and clay-water mixtures: *Soil Sci. Soc. Am. Proc.* 28, 605-609.
- Osthaus, B. B. (1956) Kinetic studies on montmorillonites and nontronites by the acid dissolution technique: *Clays Clay Miner.* 4, 301-321.
- Paver, H., and Marshall, C. E. (1934) The role of aluminum in the reactions of the clays: *J. Soc. Chem. Ind.* 53, 750- .
- Ravina, I., and Low, P. F. (1972) Relation between swelling, water properties, and b-dimension in montmorillonite-water systems: *Clays Clay Miner.* 20, 109-123.
- Ravina, I., and Low, P. F. (1977) Change of b-dimension with swelling of montmorillonite: *Clays Clay Miner.* 25, 196-200.
- Roth, C. B., Jackson, M. L., and Syers, J. K. (1969) Defferation effect on structural ferrous-ferric iron ratio and CEC of vermiculites and soils: *Clays Clay Miner.* 17, 253-264.
- Rozenson, I., and L. Heller-Kallai. (1976) Reduction and oxidation of Fe^{3+} in dioctahedral smectite. I: Reduction with Hydrazine and dithionite: *Clays Clay Miner.* 24, 271-282.
- Ruiz, H. A., and Low, P. F. (1976) Thermal expansion of interlayer water in clay systems. II. Effect of clay composition: *J. Colloid Interface Sci.* 5, 503-515.
- Russell, J. D., B. A. Goodman, and A. R. Fraser. (1979) Infrared and Mossbauer studies of reduced nontronites: *Clays Clay Miner.* 27, 63-71.
- Shainberg, I. (1973) Rate and mechanism of Na-montmorillonite hydrolysis in suspensions: *Soil Sci. Soc. Am. Proc.* 37, 689-694.
- Shainberg, I., Low, P. F., and Kafkafi, U. (1974) Electrochemistry of sodium-montmorillonite suspensions: I. Chemical stability of montmorillonite: *Soil Sci. Soc. Am. Proc.* 38, 751-756.
- Stucki, J. W. (1981) The quantitative assay of minerals for Fe^{2+} and Fe^{3+} using 1,10-phenanthroline--II: A photochemical method: *Soil Sci. Soc. Am. J.* 45, 638-641. (See also Appendix A herein)

- Stucki, J. W. and Anderson, W. L. (1981) The quantitative assay of minerals for Fe^{2+} and Fe^{3+} using 1,10-phenanthroline--I: Sources of variability: Soil Sci. Soc. Am. J. 45, 633-637. (See also Appendix A herein)
- Stucki, J. W., and C. B. Roth. (1977) Oxidation-reduction mechanism for structural iron in nontronite: Soil Sci. Soc. Am. J. 41, 808-814.
- Stucki, J. W., C. B. Roth, and W. E. Baitinger. (1976) Analysis of iron-bearing clay minerals by electron spectroscopy for chemical analysis (ESCA): Clays Clay Miner. 24, 289-292.
- Van Olphen, H. (1963) An introduction to clay colloid chemistry: Interscience, New York. 301 pp.
- Verwey, E. J. W., and Overbeek, J. Th. G. (1948) Theory of the stability of lyophobic colloids: Elsevier Publishing Co., New York. 205 pp.
- Weaver, R. M., J. K. Syers, and M. L. Jackson. (1968) Determination of silica in citrate-bicarbonate-dithionite extracts of soils: Soil Sci. Soc. Am. Proc. 32, 497-501.
- Weiss, Armin. (1958) Interlamellar swelling as a general model of swelling behavior: Chem. Ber. 91, 487-502.

APPENDIX A

The Quantitative Assay of Minerals for Fe^{2+} and Fe^{3+} Using 1,10-Phenanthroline:

I. Sources of Variability¹

J. W. STUCKI AND W. L. ANDERSON²

ABSTRACT

Factors affecting the reliability of results using 1,10-phenanthroline (phen) in the quantitative assay of minerals for Fe^{2+} and total Fe were studied. The greatest source of variability was the photochemical reduction of ferric-phen species during Fe^{2+} analyses. It is believed that oxo-bridged dinuclear complexes of Fe^{3+} and phen are formed in the mineral digests, which then are susceptible to photochemical reduction by wavelengths $< 400\text{--}500\text{ nm}$. The rate of photoreduction of a solution obtained by digesting oxidized nontronite was sufficient to increase the predicted Fe^{2+} content of the clay from about 0 to 2.45% by simply leaving the sample for 1 hour in normal fluorescent light in the laboratory; and for partially reduced nontronite, from 3.25 to 4.68%. The rates of increase for the two clays were 0.0024 and 0.0014 absorbance units/min, respectively. Interferences due to this phenomenon were eliminated when samples were kept in the dark or under subdued red light. Other factors that adversely influence the accuracy and precision of the standard curve included (i) the amount of 48% HF used to digest the sample; (ii) addition of chemical reducing agents such as hydroxylamine hydrochloride and hydroquinone; (iii) the order in which phen is added relative to other reagents; (iv) pH; and (v) the length of time allowed for color development if phen is added only to the final dilution.

Additional Index Words: photochemical reduction, hydroxylamine hydrochloride, hydroquinone, oxidation.

Stucki, J. W., and W. L. Anderson. 1981. The quantitative assay of minerals for Fe^{2+} and Fe^{3+} using 1,10-phenanthroline: I. sources of variability. *Soil Sci. Soc. Am. J.* 45:633-637.

COMPLETE characterization of the oxidation-reduction properties of iron in aluminosilicate minerals requires the ability to quantitatively assay the mineral for Fe^{2+} and Fe^{3+} simultaneously. Many methods have been published for measuring either total iron or only Fe^{2+} in various types of minerals, water, and other materials (2, 7, 8, 16, 18, 22, 25, 27). Only a very few, however, have attempted to measure both Fe^{2+} and Fe^{3+} in the same sample (4, 11, 17, 20), although numerous attempts to measure Fe^{2+} in the presence of Fe^{3+} have been reported (2, 5, 12, 14). Mössbauer spectroscopy has also been used to differentiate relative abundances of Fe^{2+} and Fe^{3+} in minerals, but the mathematical procedures required to resolve the relative intensities of the respective absorption envelopes for Fe^{2+} and Fe^{3+} involve assumptions and uncertainties that render this method generally unacceptable for quantitative analysis (10).

¹ Work supported by the Illinois Agric. Exp. Stn. and in part by the U. S. Army Res. Office. Received 10 June 1980. Accepted 19 Dec. 1980.

² Assistant Professor of Soil Chemistry and former Graduate Research Assistant, respectively.

The two analytical methods most commonly used and which appear to be the most successful for measuring Fe^{2+} and Fe^{3+} in the same mineral sample are those described by Olson (17) and Roth et al. (20). These methods use 1,10-phenanthroline (phen) as the colorimetric indicator for Fe^{2+} . Begheijn (4) recently described a method that suggests some improvements to the above methods using phen, but retains many of the same features. All of these methods measure the Fe^{2+} concentration first; then total iron is obtained after chemically reducing all of the iron to Fe^{2+} . The concentration of Fe^{3+} is subsequently calculated as the difference between Fe^{2+} and total iron concentrations. However, none of these methods takes into account the fact that Fe^{3+} in solution with phen is photochemically reduced to $\text{Fe}(\text{phen})_3^{2+}$ when exposed to light (3, 6, 15), and are thus likely to yield erroneously high values for Fe^{2+} . Indeed, for the clay mineral nontronite (API no. H33a), a ferrous content of 1.75% (24) obtained using the Roth method is considerably larger than the generally accepted value of 0.22% (19). The latter value has been verified by alternate procedures (J. D. Russell, private communication; A. D. Scott, private communication).

Nevertheless, due to their relative simplicity, sensitivity, and ability to assay a sample simultaneously for ferrous and total iron, methods using phen are very desirable. This study was therefore conceived to examine in greater detail the extent to which factors such as the photochemical reduction of ferric-phen species interfere with results for ferrous and total iron.

EXPERIMENTAL

Ferrous and total iron were measured on nontronite samples (API no. H33a) and on separate standard iron solutions prepared from reagent grade $\text{Fe}(\text{NH}_4)_2(\text{SO}_4)_6 \cdot 6\text{H}_2\text{O}$ and $\text{FeNH}_4(\text{SO}_4)_2 \cdot 12\text{H}_2\text{O}$. Procedures for Fe^{2+} and total Fe analysis included the method of Roth et al. (20) (referred to hereafter as the Roth method), and various modifications to it. The basic steps of the Roth method are summarized as follows:

Samples were dissolved by heating for 30 min in a boiling water bath in a solution containing 1 ml of 48% HF, 6 ml of 3.6N H_2SO_4 , and 1 ml of 10% 1,10-phenanthroline in 95% ethanol. The digestion tubes were removed from the water bath, and a 10 ml portion of 5% boric acid was added to remove any excess HF. The resulting solution was then diluted to 100 ml in a volumetric flask using freshly boiled water, then shaken. Ferrous iron was determined by first transferring a 10-ml aliquot of this solution to a second 100-ml volumetric flask, then adding 4 ml of a 10% solution of sodium citrate and diluting to volume with water. The absorbance was determined after 30 to 60 min at 510 nm and referred to a standard curve prepared from a ferrous standard taken through the identical procedure. The time elapsed from the beginning of dissolution to the absorbance reading varied, depending on the total number of samples being analyzed. The purpose for waiting 30 to 60 min following final dilution presumably was to allow time for full color development.

Total iron was determined by transferring a 5 ml aliquot from

the first flask to a third 100-ml volumetric flask and adding 2 ml of 10% sodium citrate. To this solution, 2 ml of 10% $\text{NH}_4\text{OH}\cdot\text{HCl}$ was added, and the entire solution was diluted to volume with freshly boiled water. The absorbance was measured at 510 nm after 24 hours and referred to ferrous standards taken through the total iron procedure. The ferric ion concentration was then calculated as the difference between total and ferrous iron.

A combination of the Roth method and the method of Olson (17) (referred to hereafter as the Roth-Olson method) was also used. This procedure was the same as the Roth method except phen was added as the last reagent in the final dilution rather than being added to the digest solution.

RESULTS AND DISCUSSION

Representative values from repeated analyses of oxidized nontronite for Fe^{2+} and total iron are given in Table 1. Mean values agree reasonably well with earlier results of Stucki et al. (24), but the precision of the Fe^{2+} determinations was very poor, giving a coefficient of variation of 5.57%. Less variation was observed in the total iron determinations where the coefficient of variation was 2.98%. These data suggest that the Roth method for measuring both Fe^{2+} and total iron is subject to considerable error, especially in the analysis for Fe^{2+} . Several factors were recognized as contributing to these observed variabilities, each of which is considered in detail below.

Photochemical Reduction of Fe^{3+}

The most obvious source of variation in the Fe^{2+} determinations was the photosensitivity of Fe^{2+} solutions when Fe^{3+} was present. This is attributed to the photochemical reduction of the ferric-phen species to $\text{Fe}(\text{phen})_3^{2+}$, the latter being the complex that is measured at 510 nm. Figure 1 illustrates the effect of light on the absorbance (at 510 nm) of solutions prepared from oxidized and partially reduced nontronite samples. When the solutions were left on the laboratory bench exposed to the overhead fluorescent lights, the absorbance increased dramatically with time in both cases. During the 1st hour, the absorbance of the oxidized sample increased from 0.003 to 0.144 at a rate of about 0.0024 A/min (absorbance units/minute); then the rate slowed to about 0.0015 A/min. After 150 min, the absorbance had reached 0.277 which corresponds to a calculated Fe^{2+} concentration in the clay of 4.83%. Since the concentration of Fe^{2+} in the clay is very low, it is obvious that a lack of precautions to prevent photoreduction can cause the Fe^{2+} content of the clay to be greatly overestimated. This explains why Stucki et al. (24) reported an erroneously high Fe^{2+} content of 1.75% for oxidized nontronite, since their analyses were performed under normal laboratory conditions with no precautions against photoreduction. It also explains why Begheijn (4) and others (9, 15, 22) were able to greatly improve the reliability of results by reducing the time for digestion and analysis to only a few minutes.

Table 1—Ferrous and total iron concentrations in oxidized nontronite determined by the method of Roth et al. (1968).

	Fe^{2+} , %	Total Fe, %
\bar{X}	1.52	24.83
SE	0.08	0.740
C.V.	5.57	2.98

The absorbance of the partially reduced sample increased at the slower rate of 0.0014 A/min. Even at this rate, however, the error becomes very large since a minimum of 1 hour is required by the Roth method before any absorbance readings can be made. During this time, the absorbance of the partially reduced sample increased from 0.190 to 0.314, which is an increase in calculated percentage in the clay from 3.25 to 4.68%, or a 44% increase. Hence, as the initial Fe^{3+} content of the clay is diminished, or the $\text{Fe}^{3+}/\text{Fe}^{2+}$ ratio is decreased, the rate of photoreduction decreases, but the errors introduced remain significant.

Equivalent solutions stored in the dark for comparable periods of time remained constant at 0 and 3.25% for the oxidized and partially reduced samples, respectively. Further studies also demonstrated that, when kept in the dark, the color intensity of these solutions was unchanged for extended periods of time (at least 1 week).

The effect of time in the light on the absorbance of standard solutions of Fe^{2+} and Fe^{3+} -phen complexes was also measured. In contrast with the above results using digested nontronite solutions, except for a slight increase due to the HF (see below), the absorbance of standard Fe^{2+} -phen solutions was unchanged by exposure to laboratory light for several hours. The photosensitivity of the standard Fe^{3+} -phen solutions was comparable to the oxidized nontronite solutions described above and illustrated in Fig. 1. The necessary conclusion is that the accurate determination of Fe^{2+} in the presence of Fe^{3+} using phen requires deliberate precautions that protect the solutions from the light. This becomes increasingly important as the initial Fe^{3+} concentration increases. The procedure for total iron is insensitive to photoreduction since addition of reducing agents converts all Fe^{3+} to Fe^{2+} .

The exact mechanism by which light affects chemical reduction of Fe^{2+} in this system is at present undetermined, but studies by Baxendale and Bridge (3) and by David et al. (6) provide sufficient information on the photoreduction of similar iron-phen systems to strongly suggest the following hypothesis. The mix-

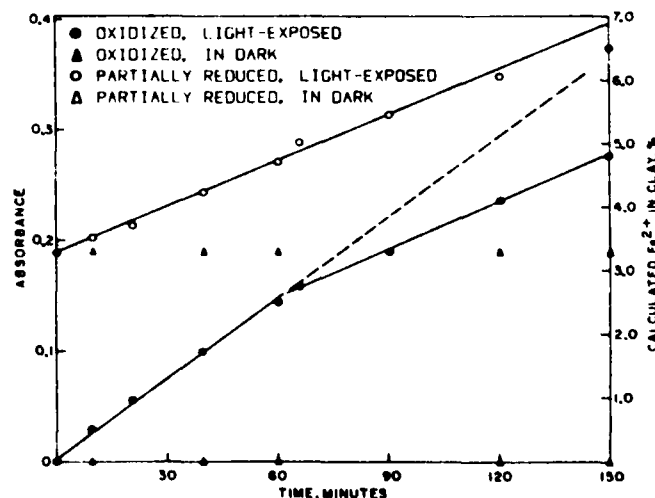
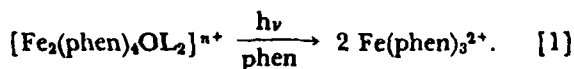


Fig. 1—The effects of normal laboratory fluorescent light on the absorbance of iron-phen solutions prepared from oxidized and partially reduced nontronite, and how these effects are reflected in the calculation of the Fe^{2+} content of the clay.

ing of phen and Fe^{3+} in solution produces the tetrakis (1,10-phenanthroline)- μ -oxodiiron(III) complex which, in the presence of light and excess phen, is reduced quantitatively by the stoichiometric reaction



The term on the left hand side of Eq. [1] is the general formula for the Fe^{3+} complex, where L is a monodentate ligand and $n = 4$ when L is a neutral species (6). The term on the right hand side is the intense red tris(1,10-phenanthroline)iron(II) complex which has an absorbance maximum at 510 nm. David et al. (6) reported significant photosensitivity of the $[\text{Fe}_2(\text{phen})_4\text{OL}_2]^{n+}$ complex to wavelengths as high as about 400 nm, depending on L and the solvent. This agrees qualitatively with results from the present study which demonstrate that wavelengths between about 300 and 500 nm induce considerable photoactivity in ferric-phen solutions. Photosensitivity was noted under both fluorescent and incandescent lighting, which emit only wavelengths greater than about 300 nm, but the same solutions were photoinactive when a red photographic lamp was used. Prolonged exposure of the ferric-phen solutions to the beam in the spectrophotometer at 510 nm induced only a very slight increase in the absorbance over several hours' time. Novak and Arend (15) also noted that ferric-phen solutions are insensitive to wavelengths > 590 nm.

Our efforts to identify the $[\text{Fe}_2(\text{phen})_4\text{OL}_2]^{n+}$ complex directly from UV-visible spectra were unsuccessful since the ferric-phen solutions prepared by the Roth method contain such an excess of phen (approximately 200 μg -phen/ml with 0. to 8- μg Fe^{3+} /ml) that the spectra were characteristic of only phen. Any contribution to the spectra by other complexes was completely masked by phen, and no differences were detected even when the Fe^{3+} concentration was varied from 0 to 8 μg /ml. This observation was unexpected since an earlier study (11) claimed that differences in the spectra of 0, 5, and 10- μg /ml Fe^{3+} in 40,000 μg /ml phen solutions are quantitatively separable.

Other studies also failed to identify the photoactive Fe^{3+} -phen complex (3, 11, 12, 14), although one (9) erroneously implied that $\text{Fe}(\text{phen})_3^{3+}$ is formed in the initial solutions when Fe^{3+} is present. The $\text{Fe}(\text{phen})_3^{3+}$ complex is prepared by oxidizing $\text{Fe}(\text{phen})_3^{2+}$ (3, 26) and is blue as compared to the faint yellow color obtained in this study. Furthermore, $\text{Fe}(\text{phen})_3^{3+}$ is photochemically reduced only by wavelengths less than about 280 nm (26), which are below the spectral ranges of either fluorescent or incandescent lighting. All evidence is, therefore, consistent with the mechanism described in Eq. [1], even though absolute spectral verification is lacking.

Addition of Reducing Agents

The variability in total iron results (Table 1) by the Roth method, although less than for Fe^{2+} , was still relatively large. It is unlikely that this is related to photochemical effects since the conversion of Fe^{3+} to Fe^{2+} by $\text{NH}_2\text{OH}\cdot\text{HCl}$ should have been complete and may be more the result of adding chemical reducing agents to the iron-phen solutions. Schilt (21) points out that erratic and nonreproducible results

Table 2—Effects of different solutes on the absorptivity of the standard solutions used in methods for total iron.

Solute added (~0.4 g)	Method	Absorptivity, ml/cm- μg					
		$\text{Fe}(\text{NH}_4)_2(\text{SO}_4) \cdot 6\text{H}_2\text{O}$			$\text{FeNH}_4(\text{SO}_4) \cdot 12\text{H}_2\text{O}$		
		n	\bar{X}	C.V.†	n	\bar{X}	C.V.†
$\text{NH}_2\text{OH}\cdot\text{HCl}$	Roth	14	0.2018	6.46	8	0.2007	5.47
Hydroquinone	Roth	3	0.2537	7.02	3	0.2564	8.17
NaCl	Roth	3	0.1965	2.51	3	0	-
$\text{NH}_2\text{OH}\cdot\text{HCl}$	Roth & Olson	5			5		
			0.1943	5.76		0.2050	4.15

† Coefficient of Variation based on the sample standard deviation.

occur if reagents are not added in this order: reducing agent, phen, citrate buffer, and, if necessary, base. His recommendation differs from the order used in the Roth procedure in that the sequence for adding reductant and phen is reversed. The procedure of the Roth-Olson method more closely adheres to Schilt's recommendation.

To test the importance of this in the total iron determinations, varying amounts of hydroxylamine hydrochloride, hydroquinone, and sodium chloride were added to solutions prepared from $\text{Fe}(\text{NH}_4)_2(\text{SO}_4) \cdot 6\text{H}_2\text{O}$ and $\text{FeNH}_4(\text{SO}_4) \cdot 12\text{H}_2\text{O}$ and treated according to both the Roth and Roth-Olson procedures. The results from the Roth method are reported in Table 2 and clearly show that the accuracy and precision of the calibration curve are diminished when salts or reducing agents are added after formation of the iron-phen complex. The results were similar regardless of whether the standard solution was Fe^{2+} or Fe^{3+} . The standard error of the mean absorptivity increased in the order $\text{NaCl} < \text{hydroquinone} \sim \text{NH}_2\text{OH}\cdot\text{HCl}$. Thus, addition of reducing agents gives the poorest results. When phen is added to iron solutions that already contain reducing agent (Roth-Olson method), the coefficient of variation of the sample standard deviation is still relatively high at the 4-6% level when using $\text{NH}_2\text{OH}\cdot\text{HCl}$.

These variations in the standard curve cannot be attributed to the oxidation of Fe^{2+} during digestion and analysis because the effect is the same regardless of whether the sample is initially Fe^{3+} or Fe^{2+} . Precisely how these solutes enhance the color intensity is unexplained. The effect becomes more pronounced as the amount of salt added is increased, and the addition of the salts as aqueous solutions does little to improve the results. Solutions containing digested samples are expected to behave similarly, although this cannot be demonstrated, due to their "unknown Fe" property.

The lack of precision in the total iron measurements reported in Table 1 may therefore be attributed in part to the effects of adding a reducing agent to the solution containing iron-phen complexes. The results in Table 2 further suggest that accurate and precise measurement of total iron using the methods of Olson (16) and Begheijn (4) may be difficult. Since the final color, however, is very sensitive to the reagents present in the solution, any extrapolation of these results to methods in which even one reagent is different should be viewed cautiously. Even though the procedures and reagents used in the methods of Olson (16) and Begheijn (4) are similar to those used in this study, no attempt was made to exactly duplicate their methods.

Hydrofluoric Acid

The effects of hydrofluoric acid on the calibration curve for ferrous iron were measured both with and without silicate, and the combined effects of light and HF were also examined. Two sets of standard ferrous solutions were prepared in six different concentrations within the range 0- to 8- μg Fe^{2+} /ml. Both sets were taken through the Roth procedure for ferrous iron, except the amount of HF added to the initial digest solutions varied from 0 to 4 ml; to one set was added 30 mg of iron-free kaolinite. For each level of HF added, two separate dilutions were made from the digestates: one was treated normally, the other was exposed to fluorescent light for 36 hours prior to measuring its absorbance. Each treatment was repeated at least twice. After each treatment, the absorptivity for each standard solution was calculated from the Beer-Lambert Law. These values were then used to calculate a mean absorptivity and standard deviation. The overall slope of the calibration curve is thus represented by the mean absorptivity and its linearity is inversely proportional to the standard deviation.

The results, reported in Table 3, indicate that variation in the quantity of HF added to the digest solution influences both the slope and the linearity of the calibration curve. When no HF was added, the curve was linear and reproducible over the concentration range studied, and light had no effect on the absorptivity. When 1 ml of HF was added in the absence of light, the mean absorptivity decreased reproducibly by about 5% but the linearity of the curve was essentially preserved. Subsequent exposure of these solutions to the light restored the absorptivity to its original value when no HF had been added. On the other hand, the addition of 2 or 4 ml of HF resulted in a large decrease (about 40%) in the absorptivity, the standard deviation increased sharply, and the curves were non-reproducible. Results obtained with and without kaolinite differed by less than their respective standard deviations and were therefore considered to be statistically equivalent.

These results suggest that the amount of HF added to the initial digest solution should not exceed 1 ml and must be the same in every sample and standard used. Further, the amount of silicate mineral that can be analyzed by these methods appears to be limited to the amount soluble by 1 ml of 48% HF.

One possible explanation for the decreased absorptivity as the result of increasing the amount of HF is that F^- competes with phen for ligand sites in the Fe^{2+}

complex, thereby diminishing the number of phen ligands complexed to Fe^{2+} . This could lower the absorptivity of the complex at 510 nm. At sufficiently large concentrations of both Fe^{2+} and F^- (about 10^2 and 10^4 $\mu\text{g}/\text{ml}$, respectively) in the digestate, a precipitate is formed that exhibits solubility properties similar to an iron fluoride complex, suggesting that F^- may be successful in displacing or competing with some of the phen. This, however, provides no ready explanation for the observed absorptivity increase when the 1-ml HF treatment is exposed to light.

An alternative explanation is that some Fe^{2+} is oxidized during digestion. This would be consistent with both the direction of the absorptivity change and the effect of light, since light reduces Fe^{3+} photochemically. While a proposal that either F^- (which is already in its lowest possible oxidation state) or H^+ would oxidize Fe^{2+} under these conditions is unreasonable, HF apparently can catalyze the air oxidation of Fe^{2+} in comparable solutions (13). The data are insufficient at this point to draw a firm conclusion as to which, if not both, of these factors are operating.

Oxidation and pH

Oxidation of Fe^{2+} to Fe^{3+} will occur if phen is absent from the digest solution. Comparison of solutions digested with and without phen revealed that the final absorptivity decreased by 8.5% when phen was absent from the digest solution, which points out the importance of having phen in the solution to which Fe^{2+} is released upon digestion. It is possible, therefore, that the Roth-Olson and the Olson (17) methods for Fe^{2+} are likewise susceptible to oxidation.

Erratic results are also obtained if the pH in the digest solution is too low. The absorptivity of ferrous standards dissolved in the presence of phen was optimized when 12 ml of 3.6N H_2SO_4 was used in the digest. The results were comparable when using 6 ml of 7.2N H_2SO_4 , but extensive oxidation occurred when the H^+ concentration dropped much below 2.9M during digestion. Subsequent dilutions to 100 ml yielded more satisfactory and reproducible results than when 50 ml was used. Presumably this is related to the pH-dependence of the color development in the final solution (20, 21), which required a pH between about 2.5 and 6.0.

Rate of Color Development

Complete color development in the final flask of the procedure is time dependent. It also varies with pH and with the order in which phen is added. When phen is added to the digest solutions, where the pH is < 0 , the color is developed rapidly and completely by the time all dilutions are made. If, however, the Roth-Olson procedure is used in which phen is not added until the final flask, where the pH is between 2 and 4, the rate is much slower, and requires at least 4 hours for full color development of an 8- $\mu\text{g}/\text{ml}$ solution of Fe^{2+} . If the analysis is intended for Fe^{2+} only, this must take place under nonphotoreducing conditions. Raising the temperature of the final solution to accelerate the rate of color formation is not recommended since the color in the final solution is unstable above about 50°C.

Table 3—The effect of 48% HF and 36 hours in fluorescent light on the mean absorptivity (\bar{X}) and sample standard deviation (S) of $\text{Fe}(\text{phen})_3^{+}$ solutions prepared by the Roth method using $\text{Fe}(\text{NH}_4)_2(\text{SO}_4)_6 \cdot 6\text{H}_2\text{O}$.

Amount of HF added to digest solution, ml	Absorptivity, \uparrow ml/cm- μg			
	Exposed to light		Kept in darkness	
	$\bar{X} \pm$	S	$\bar{X} \pm$	S
0	0.1948	0.0012	0.1962	0.0005
1	0.1960	0.0023	0.1852	0.0026
2	0.1226	0.0956	0.1217	0.0927
4	0.1001	0.0073	0.1203	0.0043

\uparrow Calculated from the Beer-Lambert law

\dagger Based on the absorptivity of six standard solutions ranging in concentration from 2 to 8- μg Fe^{2+}/ml solution.

SUMMARY AND CONCLUSIONS

Methods for measuring Fe^{2+} and Fe^{3+} in minerals using 1,10-phenanthroline are subject to numerous sources of variability, the most pronounced of which is the photochemical reduction of ferric-phen species to $\text{Fe}(\text{phen})_3^{2+}$. When samples containing Fe^{3+} are assayed for Fe^{2+} only, erroneously high values are obtained if the analysis is performed in the light. This effect is completely eliminated by performing the analyses under subdued red light or in complete darkness. If phen is deleted from the initial digest solution, appreciable oxidation is observed in both the ferrous standards and the samples.

The precision and accuracy of standard curves prepared from either Fe^{2+} or Fe^{3+} salts are adversely affected when chemical reducing agents are added. The effect is greatest when the iron-phen complexes are allowed to form prior to addition of the reducing agent. This is a difficult problem and seems to exist regardless of the redox properties of the salt added. It thus detracts from the integrity of total iron analyses by 1,10-phenanthroline methods. An alternative means for reducing the iron to obtain total iron, however, may be found by exploiting the photochemical properties of the ferric-phen complexes that are formed. This concept is explored in depth in another study (23).

ACKNOWLEDGMENT

The authors would like to thank Rose Pilgrim for her very able laboratory assistance.

LITERATURE CITED

1. Allan, J. E. 1959. The determination of iron and manganese by atomic absorption. *Spectrochim. Acta*. 15:800-806.
2. American Public Health Association. 1976. Standard methods for the examination of water and wastewater. 14th ed. APHA/AWWA/WPCF. Washington, DC.
3. Baxendale, J. H., and N. K. Bridge. 1955. The photoreduction of some ferric compounds in aqueous solution. *J. Phys. Chem.* 59:783-788.
4. Begheijn, L. T. 1979. Determination of iron(II) in rock, soil, and clay. *Analyst (London)* 104:1055-1061.
5. Cronheim, G., and W. Wink. 1942. Determination of divalent iron. *Ind. Eng. Chem.* 14:447-448.
6. David, P. G., J. G. Richardson, and E. L. Wehry. 1972. Photoreduction of tetrakis(1,10-phenanthroline)- μ -oxodiiron (III) complexes in aqueous and acetonitrile solution. *J. Inorg. Nucl. Chem.* 34:1333-1346.
7. Fishman, M. J., and D. E. Erdmann. 1979. Water analysis. *Anal. Chem.* 51:317R-341R.
8. Fortune, W. B., and M. G. Mellon. 1938. Determination of iron with o-phenanthroline. A spectrophotometric study. *Ind. Eng. Chem., Anal. Ed.* 10:60-64.
9. Ghosh, A. R., and I. I. Radhakrishnan. 1967. Limitations in the determination of ferrous iron by orthophenanthroline method. *J. Inst. Chemists (Calcutta)* 34:168-172.
10. Goodman, B. A. 1980. Mössbauer spectroscopy. p. 1-92. In J. W. Stucki and W. L. Banwart (ed.) *Advanced chemical methods for soil and clay minerals research*. D. Reidel Publishing Co., Dordrecht, Holland.
11. Harvey, A. E., Jr., J. A. Smart, and E. S. Amis. 1955. Simultaneous spectrophotometric determination of iron(II) and total iron with 1,10-phenanthroline. *Anal. Chem.* 27:26-29.
12. Heaney, S. I., and W. Davison. 1977. The determination of ferrous iron in natural waters with 2,2'-bipyridyl. *Limnol. Oceanogr.* 22:753-760.
13. Hillebrand, W. F., G. E. F. Lundell, H. A. Bright, and J. I. Hoffman. 1953. *Applied inorganic analysis*. 2nd ed. John Wiley & Sons, New York.
14. Lee, G. F., and W. Stumm. 1960. Determination of ferrous iron in the presence of ferric iron with bathophenanthroline. *J. Am. Water Works Assoc.* 52:1567-1574.
15. Novak, J., and H. Arend. 1964. The photosensitivity of the complex of iron(III) with 1,10-phenanthroline. *Talanta* 11:898-899.
16. O'Connor, J. T., K. Komolrit, and R. S. Engelbrecht. 1965. Evaluation of the orthophenanthroline method for ferrous iron determination. *J. Am. Water Works Assoc.* 57:926-934.
17. Olson, R. V. 1965. Iron. In C. A. Black et al., (ed.) *Methods of soil analysis*, part 2. Agronomy 9:963-973. Am. Soc. of Agron., Madison, Wis.
18. Peters, von Arnd. 1968. Ein neues verfahren zur bestimmung eisen (II) oxide in mineralen und gesteinen. *Neues Jahrb. Mineral. Monatsh.* 3/4:119-125.
19. Ross, C. S., and S. B. Hendricks. 1945. Minerals of the montmorillonite group. Their origin and relation to soils and clays. U. S. Geol. Survey, Prof. Paper 205B:23-79. U.S. Government Printing Office, Washington, DC.
20. Roth, C. B., M. L. Jackson, E. G. Lotse, and J. K. Syers. 1968. Ferrous-ferric ratio and C.E.C. changes on deferration of weathered micaceous vermiculites. *Isr. J. Chem.* 6:261-273.
21. Schilt, A. A. 1967. *Analytical applications of 1,10-phenanthroline and related compounds*. Pergamon Press, New York.
22. Shapiro, L. 1960. A spectrophotometric method for the determination of FeO in rocks. *Geol. Survey Res.* 1960: B496-B497.
23. Stucki, J. W. 1981. The quantitative assay of minerals for Fe^{3+} and Fe^{2+} using 1,10-phenanthroline. II. a photochemical method. *Soil Sci. Soc. Am. J.* 45:638-641 (this issue).
24. Stucki, J. W., C. B. Roth, and W. E. Baitinger. 1976. Analysis of iron-bearing clay minerals by electron spectroscopy for chemical analysis (ESCA). *Clays Clay Miner.* 24:289-292.
25. Tackett, S. L., and M. A. Brocius. 1969. X-ray fluorescence determination of iron in polluted streams. *Anal. Lett.* 2: 649-655.
26. Wehry, E. L., and R. A. Ward. 1971. Photoreduction of tris(1,10-phenanthroline)iron(II). *Inorg. Chem.* 10:2660-2664.
27. Wilson, A. D. 1960. The microdetermination of ferrous iron in silicate minerals by volumetric and colorimetric methods. *Analyst (London)* 85:823-827.

The Quantitative Assay of Minerals for Fe^{2+} and Fe^{3+} Using 1,10-Phenanthroline: II. A Photochemical Method¹

J. W. STUCKI²

ABSTRACT

A photochemical method for measuring Fe^{2+} and total Fe in minerals is described. The method determines Fe^{2+} concentration by measuring the $\text{Fe}(\text{phen})_3^{2+}$ (phen = 1,10-phenanthroline) complex formed during $\text{HF-H}_2\text{SO}_4$ digestion of the mineral. To measure Fe^{2+} accurately in the presence of Fe^{3+} from the mineral, the sample digestion and analysis are performed under red light to prevent photochemical reduction of the ferric-phen species. Total iron is measured by converting any Fe^{2+} in the digestate to $\text{Fe}(\text{phen})_3^{2+}$ by photochemical reduction using a fluorescent lamp. This procedure avoids the problems associated with adding chemical reducing agents to iron-phen solutions. The calibration curves were linear up to $8\text{-}\mu\text{g Fe/ml}$ with a lower detection limit of $0.011\text{ }\mu\text{g/ml}$. The absorptivities of the calibration curves were 0.1852 ± 0.0017 and $0.1960 \pm 0.0018\text{ ml/cm}\cdot\mu\text{g}$ for Fe^{2+} and total Fe, respectively. Ferric iron in the mineral samples was calculated by difference.

Additional Index Words: iron assay.

Stucki, J. W. 1981. The quantitative assay of minerals for Fe^{2+} and Fe^{3+} using 1,10-phenanthroline: II. A photochemical method. *Soil Sci. Soc. Am. J.* 45:638-641.

STUCKI AND ANDERSON (9) report that the use of 1,10-phenanthroline (phen) to measure both Fe^{2+} and total Fe in minerals is subject to considerable error due primarily to two factors: the photochemical reduction of Fe^{3+} , and the color instability as a result of adding chemical reducing agents to solutions containing iron-phen complexes.

The precision of total iron results is adversely affected by the addition of chemical reducing agents after the iron-phen complexes have formed. The coefficients of variation (C.V.) for the absorptivity of $\text{Fe}(\text{NH}_4)_2(\text{SO}_4)_2 \cdot 6\text{H}_2\text{O}$ standard solutions were 14.88 and 7.01% when hydroxylamine hydrochloride and hydroquinone were added, respectively. However, in a series of analyses of nontronite for total iron using hydroxylamine hydrochloride as the reducing agent, C.V. was only 2.98% (9), suggesting that other compensating errors exist. The relatively good precision of this result appears to be fortuitous, and the poor reproducibility of the standard curve indicates a need for better precision. Since none of the currently available methods that rely on phen to measure both Fe^{2+} and total Fe account for these sources of variability, a new method is needed. When phen is added to a solution containing Fe^{3+} , a dinuclear ferric-phen complex is formed (2). Upon exposure to light of wavelengths $< 500\text{ nm}$ (approximately), this complex is photochemically reduced to $\text{Fe}(\text{phen})_3^{2+}$, the intensely colored complex that is measured colorimetrically at 510 nm . Thus, in a mineral sample that contains some Fe^{3+} , the amount of Fe^{2+} measured by phen will be higher than the true value if the sample solution is

exposed to light. The magnitude of this error increases with the intensity of the light and with exposure time (9).

The phenomenon common to the procedures for Fe^{2+} and for total iron is the photochemical reduction of ferric-phen complexes—a detriment that must be eliminated in the case of Fe^{2+} determinations and an asset that may substitute for the addition of chemical reducing agents in the total iron procedure. The possibility that photoreduction can substitute for chemical reducing agents is indicated by the observations of David et al. (2) that ferric-phen complexes are quantitatively and stoichiometrically reduced to $\text{Fe}(\text{phen})_3^{2+}$ in the presence of excess phen. The purpose of this paper is to describe a photochemical method based on the method of Roth et al. (6) for Fe^{2+} and Fe^{3+} determination in minerals that exploits the photosensitivity of ferric-phen solutions. It also accounts for the variability described earlier (9) due to oxidation, pH, rate of color formation, and the presence of HF acid.

EXPERIMENTAL

Materials

Minerals—Mineral samples used in this study are listed in Table 1 along with their origins and descriptions. The USGS mineral standards were used directly as supplied, and nontronite was prepared as described by Stucki et al. (10).

Reagents—1,10-phenanthroline monohydrate in 95% ethanol as a 10% (wt/wt) solution; 3.6N sulfuric acid; 48% HF acid; 5% (wt/wt) boric acid solution in water; 10% (wt/wt) sodium citrate dihydrate in water; and reagent-grade $\text{Fe}(\text{NH}_4)_2(\text{SO}_4)_6 \cdot 6\text{H}_2\text{O}$ (ferrous ammonium sulfate hexahydrate salt). All water used was deionized to 18 megohm resistivity, using a Millipore milli-Q water purification system.

Apparatus—Boiling water bath with a container to hold 100-ml centrifuge tubes; 100-ml polypropylene centrifuge tubes; 1-ml Eppendorf pipet with plastic tips; 50-ml pyrex Erlenmeyer flasks with rubber stoppers; a dual circline lamp fixture equipped with one 20-cm (8-inch) diameter (22 W) and one 30.5-cm (12-inch) diam (40 W) circular fluorescent bulbs, inverted and covered with a 0.125-inch thick sheet of pyrex glass; a Beckman model 5230 UV-visible spectrophotometer capable of a linear absorbance range of at least 0 to 2, a three-decimal absorbance display, and a flow-through cell with sipper accessory; a desk lamp with a red bulb; a top-loading balance accurate to $\pm 0.01\text{ g}$; and an automatic dilutor capable of 1:10 dilution ratios (preferably 1 ml:10 ml capacities) with an overall precision better than $\pm 0.3\%$. In this study, the pipet portion of the dilutor was calibrated with distilled water to transfer $0.803 \pm 0.0023\text{ g}$ and to dilute with $7.2199 \pm 0.0148\text{ g}$.

Recommended Method

Procedure—Ferrous and total iron were determined by adding 25–50 mg of dried mineral sample containing $< 7.5\text{ mg}$ of total iron to a 100-ml polypropylene centrifuge tube. The room was then darkened and the red lamp turned on to illuminate the work area. The sample was digested by adding 12 ml of 3.6N H_2SO_4 , 2 ml of 10% phen, and 1 ml of 48% HF (using the plastic Eppendorf pipet) to the tube, in that order; this, in turn, was placed unstoppered into the boiling water bath. After exactly 30 min the tube was removed from the bath and cooled at room temperature for 15 min. Ten ml of boric acid was added. Using the top-loading balance, the solution was diluted gravimetrically to about 80 to 90 g and converted directly to volume units since the density was 1.005 at 24°C . The tube was then covered with parafilm, and its contents were

¹ Work supported by the Ill. Agric. Exp. Stn. and the U. S. Army Res. Office. Received 8 July 1980. Approved 19 Dec. 1980.

² Assistant Professor of Soil Chemistry, Dep. of Agron., Univ. of Illinois, Urbana, IL 61801.

mixed thoroughly. This solution was protected from the room light at all times.

With the red lamp still on and using the automatic dilutor, one aliquot (0.803 g) from the sample tube was transferred immediately to each of two 50-ml Erlenmeyer flasks containing 1 aliquot (0.803 g) of 10% sodium citrate, and diluted with water. The absorbance of the solution in the first flask was measured immediately at 510 nm. The second flask was stoppered and placed on the fluorescent lamp for 36 hours and the absorbance of this solution measured after allowing it to cool for 2 to 3 min. These absorbance values were substituted into Eq. [2] to calculate ferrous and total iron concentrations, respectively.

Calibration Curves—Calibration curves were prepared by treating $\text{Fe}(\text{NH}_4)_2(\text{SO}_4)_2 \cdot 6\text{H}_2\text{O}$ exactly according to the procedures described above for ferrous and total iron. Reagent blank solutions, which contained all reagents except the iron salt, were also prepared in like manner. Using the dilution ratios described above, each 7-mg portion of $\text{Fe}(\text{NH}_4)_2(\text{SO}_4)_2 \cdot 6\text{H}_2\text{O}$ added to the digestion tube resulted in about 1 $\mu\text{g-Fe/ml}$ in the final flask.

Calculations—The absorptivities of the standard solutions, denoted ϵ , were calculated for iron concentrations ranging between 0 and 8 $\mu\text{g/ml}$ using the Beer-Lambert Law, namely:

$$\epsilon_s = (A_s - A_b)/lc, \quad [1]$$

where A_s and A_b are the absorbances of the standard and reagent blank solutions, respectively; l , the path length (1 cm); and c , the Fe concentration in $\mu\text{g/ml}$.

The concentrations of ferrous and total iron were calculated from the equation

$$c_i = \frac{(A_i - A_b) V_s' V_d}{\epsilon_i m_s V_A} 10^{-4}, \quad [2]$$

where c_i is the weight percent of Fe (either ferrous or total iron) in the mineral; A_i , the absorbance of the unknown solution (either ferrous or total iron); m_s , the mass of mineral sample added to the sample tube, in grams; V_s' , the diluted volume of the sample tube; V_d , the total volume of the solution in the final flask; and V_A , the volume of the aliquot transferred from the sample tube to the final flask. The density of the solution in the final flask was 1.0042 g/cm^3 ; no density correction was therefore used in converting the solution weight to volume, i.e., a density of 1 g/cm^3 was used.

The weight percent of Fe^{2+} in the sample was calculated simply as the difference between total and ferrous iron.

Comparative Methods

Ferrous and total iron were also determined by alternative methods which served as a basis for comparison of results. Ferrous iron was measured in nontronite and PCC-1 using a vanadyl titration procedure described by A. D. Scott (private communication), based on the method of Peters (5). Total iron was measured on all samples by atomic absorption at 589 nm using a Perkin-Elmer Model 5000 spectrophotometer and an air-acetylene flame. These solutions consisted of a 1:30 dilution of the digestates in the 100-ml polypropylene tubes prepared by the photochemical method described above.

RESULTS AND DISCUSSION

The calibration curves for ferrous and total iron using $\text{Fe}(\text{NH}_4)_2(\text{SO}_4)_2 \cdot 6\text{H}_2\text{O}$ were linear up to 8- $\mu\text{g Fe/ml}$ with mean absorptivities of 0.1852 ± 0.0017 and 0.1960 ± 0.0018 $\text{ml/cm-}\mu\text{g}$, respectively, for the 99% confidence interval. The lower detection limit was 0.011- $\mu\text{g Fe/ml}$. As these values indicate, the standard curves were easily reproduced with high precision and linearity, which in the case of total iron is an improvement over the values obtained by Stucki and Anderson (9) using hydroxylamine hydrochloride as a reducing agent. The above absorptivity values, which are a property of the absorbing solution alone and thus independent of the instrument used to measure their absorbance, should serve as a guide to evalu-

Table 1—Mineral samples studied.

Mineral	Description	Source
AGV-1	Andesite	USGS Split 62, position 8
GSP-1	Granadiorite	USGS Split 27, position 11
G-2	Granite	USGS Split 74, position 14
PCC-1	Peridotite	USGS Split 76, position 14
Nontronite	API H33a, < 2 μm , Na-saturated	Wards Natural Science Establishment
Biotite	< 2 μm Bancroft, Ontario	Wards Natural Science Establishment
Vermiculite	Heterogeneous	Unknown

Table 2—Percent ferrous and total iron in selected mineral samples determined by the photochemical method as compared to other methods.

Mineral	Method		Flanagan (1967)	Carmichael et al. (1968)
	This study†			
	Photochemical	Other‡		
<u>Ferrous Iron</u>				
AGV-1	1.65 (0.32)	n.d.§	1.56	1.61
GSP-1	1.77 (0.61)	n.d.	1.74	1.84
G-2	1.29 (7.24)	n.d.	1.43	1.17
PCC-1	4.12 (0.58)	4.18	3.79	4.02
Nontronite	0.05 (30.40)	~0	n.d.	n.d.
Biotite	11.44 (0.51)	n.d.	n.d.	n.d.
Vermiculite	1.29 (0.55)	n.d.	n.d.	n.d.
<u>Total Iron</u>				
AGV-1	4.57 (0.44)	4.70 (0.18)	4.65	4.69
GSP-1	2.40 (0.75)	2.45 (0.09)	3.04	2.97
G-2	1.86 (4.44)	1.72 (0.06)	1.89	1.84
PCC-1	5.22 (0.94)	5.36 (0.17)	5.75	5.70
Nontronite	24.04 (0.54)	24.32 (1.00)	n.d.	n.d.
Biotite	13.90 (0.49)	13.93 (n.d.)	n.d.	n.d.
Vermiculite	6.57 (0.73)	6.60 (0.16)	n.d.	n.d.

† Numbers in () are the coefficient of variation (C.V.) based on the standard error of the mean (SE).

‡ Ferrous determined by Scott's method; and total iron by atomic absorption using the digestates prepared in the photochemical method.

§ n.d. = not determined.

ate the integrity of calibration curves determined with any visible wavelength absorption photometer.

The difference in the absorptivities of the ferrous and total iron standards is attributed entirely to the presence of HF acid, which decreases the slope of the ferrous curve depending on the amount of HF added (9). The addition of 1 ml or less of HF yields satisfactory results. Even though the absorptivity is slightly less than when no HF is added, quantities > 1 ml result in poor reproducibility and precision. For these reasons, the amount of HF added to the digest solutions must be the same for each sample and standard used and should not exceed 1 ml. This imposes an inherent limitation on the amount of silicate mineral that can be dissolved and subsequently analyzed for Fe^{2+} and Fe^{3+} using the photochemical method as described above.

That HF is partially consumed by the silicate samples during digestion, and because the standards contained no silicate, perhaps the effect of F^- on the observed absorptivity for the standards will be less pronounced in the samples. To test this possibility, 0, 1-, 2- or 4-ml aliquots of 48% HF and 30 mg of iron-free kaolinite were added in triplicate to each of several solutions representing a 2-8 $\mu\text{g/ml}$ concentration range, and their respective absorptivities and standard deviations were measured. The results did not differ significantly (at the 99% CI) from the values reported

above when kaolinite was absent, so any error introduced by preparing the standard solutions without adding a silicate was negligible.

In Table 2 the Fe^{2+} and total Fe results for selected mineral samples (described in Table 1) using the photochemical method are compared with values reported by Flanagan (3) and Carmichael et al. (1), and with results obtained in this study using atomic absorption for total Fe and vanadyl titration for Fe^{2+} . The precision of the photochemical method is excellent as indicated by the low (<1%) C.V. for most samples. The results for total iron are within 1 to 2% of those obtained by atomic absorption and generally agree with the iron assays of the USGS mineral standards reported by others (1, 3). This close agreement in total iron values demonstrates that photochemical reduction is an accurate and effective alternative to chemical reducing agents as a means for determining total iron with phen.

The most obvious discrepancy in the USGS samples is in the case of GSP-1 where the photochemical method measured 20% less total iron than either of the other two studies (1, 3). However, the fact that atomic absorption confirms the photochemical results suggests that the particular sample of GSP-1 used in this study may be somewhat different from that used by Carmichael et al. (1) and Flanagan (3). Also, standard deviation information is lacking in the latter studies so no test for statistically significant differences could be made. The problems of solubility of PCC-1 described by Carmichael et al. (1) also apply to the photochemical method and perhaps explain some of the discrepancy seen in this case.

As for Fe^{2+} analyses, the amounts measured in the USGS standards by all methods were comparable, and certainly within the limits of variation that might be expected from one study to another. The accuracy of the photochemical results lies within the range of variability observed between the values reported by Flanagan (3) and Carmichael et al. (1).

Results for nontronite using the photochemical method (Table 2) were also compared with previously published results (7, 10) where the Roth method (6) had been used. The total iron content of 24.04% (Table 2) agreed quite well with the earlier results of 24.86% (10) and 24.74% (7); but the Roth method greatly overestimated the Fe^{2+} composition of oxidized nontronite, giving values of 1.75% and 2.79% compared to only a trace (<0.05%) by the photochemical and vanadyl titration methods. These discrepancies are directly attributable to the photoreduction of Fe^{3+} during Fe^{2+} analysis using the Roth procedure, since no precautions were taken in those studies to protect the solutions from the light. This accounts fully for the erroneously high values reported for the Fe^{2+} content of nontronite and probably also explains why the result from Stucki et al. (10) does not exactly agree with that of Roth et al. (7).

The recommended pH range of the final solution is about 2.5 to 4.0 (8). Small (0.5) deviations beyond these limits, achieved by varying the concentration of the citrate solution, seemed to have little or no effect on the final results obtained in this study.

Experience has shown that failure to rigorously follow the prescribed method often yields unsatisfactory results. It is therefore recommended that all pos-

sible sources of variability be considered carefully before modifications are introduced routinely.

Oxidation of Fe^{2+} to Fe^{3+} is absent during the entire procedure as long as phen is present and the pH of the digest solution is low (<2). If left in the diluted digestion tube for more than a few hours, the measured level of total iron in the solution decreases steadily. Possible reasons for this deterioration in the apparent concentration of total Fe are discussed elsewhere (9) but seem to be linked with the reaction of F^- with Fe^{3+} , Fe^{2+} , or both (4). The mechanism of interference may include either oxidation due to the low dissociation of FeF_3 complexes (4) or simply ligand exchange on the $\text{Fe}(\text{phen})_3^{2+}$ complex. Once the pH has been buffered to 2.9 to 4.0, the solution in the final flask is stable for at least one week. Solutions intended for Fe^{2+} analysis must be stored in the dark.

CONCLUSIONS

The photochemical method described above offers several improvements over the Roth method (7) in the quantitative assay of minerals for Fe^{2+} and Fe^{3+} . These are:

- 1) Fe^{2+} can be measured accurately in the presence of Fe^{3+} , regardless of their relative ratios.
- 2) Photochemical reduction, rather than the addition of chemical reducing agents to the iron-phen solutions, yields high precision in the total iron calibration curve, thus making possible a more reliable result.
- 3) The opportunity for dilution errors is diminished by using an automatic dilutor and by diluting the digested solutions directly in the tubes rather than transferring to a volumetric flask.
- 4) The use of an automatic dilutor decreases tedium and facilitates the analysis of more samples and replicates in a shorter period of time, thus enhancing the opportunity to check precision. The total time required to analyze 16 samples in triplicate is reduced to 2 hours.

The principal limitation to this method is that it has been tested and evaluated specifically for only those samples that can be digested using $\text{HF-H}_2\text{SO}_4$. However, there is no a priori reason to exclude alternative digestion media, provided that adequate calibration is achieved, the principles for dealing with photochemical reduction are applied properly, and the final pH range of 2.9 to 4.0 is maintained. These same criteria should also be applied to evaluate any modification that may become desirable.

ACKNOWLEDGMENT

The author would like to acknowledge and thank Rose Pilgrim for laboratory assistance and Dhanpat Rai for supplying the samples of biotite and vermiculite.

LITERATURE CITED

1. Carmichael, I. S. E., J. Hampel, and R. N. Jack. 1968. Analytical data on the U. S. G. S. standard rocks. *Chem. Geol.* 3:59-64.
2. David, P. G., J. G. Richardson, and E. L. Wehry. 1972. Photoreduction of tetrakis(1,10-phenanthroline) μ oxoduron (III) complexes in aqueous and acetonitrile solution. *J. Inorg. Nucl. Chem.* 34:1333-1346.
3. Flanagan, E. J. 1967. U. S. Geological Survey silicate rock standards. *Geochim. Cosmochim. Acta* 31:289-308.
4. Hillebrand, W. F., G. E. F. Lundell, H. A. Bright, and J. I. Hoffman. 1953. *Applied inorganic analysis*. 2nd ed.

- John Wiley & Sons, New York.
5. Peters, von Arnd. 1968. Ein neues verfahren zur bestimmung eisen (II) oxide in mineralen und gesteinen. Neues Jahrb. Mineral. Monatsh. 3/4:119-125.
 6. Roth, C. B., M. L. Jackson, E. G. Lotse, and J. K. Syers. 1968. Ferrous-ferric ratio and C.E.C. changes on deferration of weathered micaceous vermiculites. Isr. J. Chem. 6:261-273.
 7. Roth, C. B., M. L. Jackson, and J. K. Syers. 1969. Deferration effect on structural ferrous-ferric iron ratio and CEC of vermiculites and soils. Clays Clay Miner. 17:253-264.
 8. Schilt, A. A. 1967. Analytical applications of 1,10-phenanthroline and related compounds. Pergamon Press, New York.
 9. Stucki, J. W., and W. L. Anderson. 1980. The quantitative assay of minerals for Fe^{2+} and Fe^{3+} using 1,10-phenanthroline: I. sources of variability. Soil Sci. Soc. Am. J. 45:633-637 (this issue).
 10. Stucki, J. W., C. B. Roth, and W. E. Baitinger. 1976. Analysis of iron-bearing clay minerals by electron spectroscopy for chemical analysis (ESCA). Clays Clay Miner. 24:289-292.

APPENDIX B

On August 22, 1979, Philip F. Low, Charles B. Roth, and Joseph W. Stucki filed a record and disclosure of invention form with the Purdue Research Foundation under the title "Method for rapid beneficiation of bentonite (smectite) clays." This disclosure occurred prior to the initiation of this project with the Army Research Office, and was based on the earlier reports and observations of the inventors. Later, on August 4, 1981, this record and disclosure was up-dated with some of the data collected as part of this project. Then in December, 1981, a formal Application for Patent was filed with the U. S. Patent Office by the Purdue Research Foundation. As of this date the application is still pending.

FILMED

5-83

DTIC